








## Gold particle chemistry and vein architecture in the Serrita–Salgueiro District, Western Transversal Zone of the Borborema Province, Brazil

Stella Bijos Guimarães<sup>1\*</sup> , Geysson de Almeida Lages<sup>2,4</sup> , André Luiz Carneiro Cunha<sup>2</sup> ,  
Douglas Almeida Silveira<sup>3</sup> , Felipe José da Cruz Lima<sup>2</sup> 

<sup>1</sup>Geological Survey of Brazil. SBN, Quadra 2, Bloco H, 1º andar, Brasília-DF, Brazil, CEP: 70040-904.

<sup>2</sup>Geological Survey of Brazil. Avenida Sul, 2291, Bairro Afogados, Recife-PE, Brazil, CEP: 50770-011.

<sup>3</sup>Geological Survey of Brazil. Avenida Brasil, 1731, Funcionários, Belo Horizonte-MG, Brazil. CEP: 30140-002

<sup>4</sup>Institute of Geosciences, Universidade Estadual de Campinas, Campus Universitário, Campinas-SP, Brazil, CEP: 13083-855.

### Abstract

Gold occurrences are distributed across the Serrita–Salgueiro District in the Western Transversal Zone, Borborema Province, Brazil. Host rocks include sulfide-bearing quartz veins in metasedimentary units of the Salgueiro Complex and quartz-monzodiorites, granodiorites, and tonalites of the Serrita Suite. In both areas, gold is hosted in quartz veins arranged in extensional fractures, sheeted veins, and hydrothermal breccias. These veins are 0.1–1.5 m thick, vertical to subvertical, and oriented dominantly NW–SE, with E–W, NE–SW, and NNW–SSE sets also present. In Salgueiro, gold occurs both free in quartz and as inclusions in pyrite, chalcopyrite, and arsenopyrite, with hematite and martite subordinated; in Serrita, gold is associated with pyrite, chalcopyrite, centimeter-scale galena, and locally Hg-bearing electrum. Gold particles from Salgueiro show Au = 44–92.5 wt% and Ag = 6.8–51.5 wt%; in Serrita, Au = 74.4–94.7 wt% and Ag = 6–22 wt%. Fineness ranges from 770 to 930 (average 875) in Serrita and from 461 to 930 (average 707) in Salgueiro. Potassic to phyllic-like K-feldspar–muscovite ± fluorite halos adjacent to granites indicate F-rich magmatic–hydrothermal inputs, whereas major shear zones and chlorite–carbonate ± sericite ± cordierite halos in metasediments are consistent with shallow orogenic conditions. Taken together, we propose a mixing-dominated model in which magmatic–hydrothermal fluids exsolved from reduced intrusions interacted with metamorphic–orogenic fluids in epizonal conditions to precipitate gold.

### Article Information

Publication type: Research papers

Received 24 April 2025

Accepted 23 October 2025

Online pub. 24 October 2025

Editor: Henri Masquelin

#### Keywords:

Gold

Hydrothermal fluids

Cachoeirinha-Salgueiro-Gravatá

Metallogenic Province

Mineralization

\*Corresponding author

Stella Bijos Guimarães

E-mail address: [stella.guimaraes@sgb.gov.br](mailto:stella.guimaraes@sgb.gov.br)

### 1. Introduction

Orogenic gold deposits form during compressive to transpressive deformation processes at convergent plate margins, particularly in accretionary and collisional orogenies (Groves et al. 1998). These deposits occur mainly within deformed metamorphic blocks, which are typically located at mid-crustal levels, particularly in spatial association with significant structures, such as large-scale shear zones, within the Earth's crust (Goldfarb et al. 2001). On the other hand, magmatic-hydrothermal deposits such as Reduced Intrusion-Related Gold Systems (RIRGS) comprise various mineral deposit styles with an Au–Bi–Te–W metal assemblage, including skarns, replacements, and veins within the hydrothermal influence zone around the causative pluton. Proximal Au–W–As and distal Ag–Pb–Zn metal associations form a zoned mineral system (Hart 2007). They form in a tectonic setting

characterized by weak post-collisional extension and are associated with distinct magma types, including I, S, and A granitoids (Hart 2007).

In this context, the Borborema Province is a geological region with a history that spans various tectonic and magmatic events that have influenced and favored the occurrence of both orogenic and RIRGS gold mineralizations. Lastly, the area experienced significant orogenic processes during the Neoproterozoic, including multiple collisional and accretionary episodes. These events led to a network of deep-seated shear zones and subsidiary structures that extend into major mobile belts in Africa (Santos and Medeiros 1999; Brito Neves et al. 2000; Archanjo et al. 2008; Santos et al. 2017). Additionally, post-collisional magmatism, primarily through the intrusion of transitional granitoids (monzogranites to monzonites) within high-K calc-alkaline to shoshonitic suites, further shaped the province's geological features that favor the generation of



RIRGS deposits. These suites are associated with K-diorites exhibiting characteristics of type I granites, which were intruded between 595 and 576 Ma (Guimarães et al. 2004; Van Schmus et al. 2011). The intraplate granites, dated to be around 570 Ma and younger, with distinctive geochemical characteristics, reflect the ongoing geological development of the Borborema Province (Van Schmus et al. 2011; Guimarães et al. 2004).

Gold mineralization is heterogeneously distributed in Precambrian rocks throughout the Borborema Province, with notable occurrences of gold deposits in skarns associated with W-Mo-Bi-Te in the Seridó Belt (e.g., Bodó and Bonfim mines; Souza Neto et al. 2008; Hollanda et al. 2017), and orogenic gold deposits associated with strike-slip shear zones (e.g., São Francisco Mine; Araújo et al. 2002; Costa and Dantas 2018), orogenic gold deposits in quartz veins in the Piancó-Alto Brígida Domain, Transversal Zone genetically linked to large-scale shear zones (e.g., Itapetim Mine; Coutinho 1994; Coutinho and Aderton 1998; Santos et al. 2014); Cu-Au deposits in mafic-ultramafic rocks in the Rio Coruripe Domain (e.g. Serrote da Laje Mine; Horbach and Marimon 1988; Figueiredo 1995; Canedo 2016); and the presence of an Au-Te-Ag association in the Tróia Massif, Ceará Central Domain (e.g. Serra da Pipoca greenstone belt; Lopez 2012; Costa 2018; Costa et al. 2019).

The Serrita-Salgueiro District of the Cachoeirinha-Salgueiro Gravata Metallogenic Province (Beurlen 1995; Santos et al. 2014; Klein et al. 2024) is situated in the western part of Pernambuco State. It belongs to the Piancó-Alto Brígida Terrane (PAB) in the Transversal Zone (Figure 1). Gold discoveries in this district have increased significantly in recent years, particularly in the Salgueiro area, which is less studied than the Serrita area, where extensive research has been conducted since the 1980s.

The deposits found in this domain until now are attributed to the circulation of hydrothermal fluids associated with the final phases of ductile deformation and declining regional metamorphism culminating in the formation of Au deposits in second-order shear zones onwards (Coutinho 1994; Coutinho and Alderton 1998; Marinho and Gomes 2013; Almeida et al. 2024). In the Salgueiro area, prospecting and small-scale mining activities have been ongoing for the last decade, and there are recent targets for geological and metallogenetic studies (see Silva et al. 2024; Noronha et al. 2024; Silva 2023). On the other hand, the Serrita area of the district has been the subject of mineral deposit identification studies since the 1980s (Torres and Santos 1983; Torres et al. 1986; Mont'Alverne et al. 1995; Beurlen et al. 1997; Marinho and Gomes 2013; Brito and Marinho 2017; Cruz 2015). Estimation of 345 Kt ROM @ 11g/t Au/t (Beurlen et al. 1997).

This work aims to present petrographic data from quartz veins and mineral chemistry of gold particles from the Salgueiro area (Algodões deposit) and the contiguous Serrita area (Barra Verde deposit). The results enable us to contribute to an enhanced understanding of the genesis of gold in the Serrita-Salgueiro District, providing clues about both magmatic and non-magmatic-hydrothermal contributions.

## 2. Geological setting

The Borborema Province in northeastern Brazil has a geological history spanning from the Archean to the

Phanerozoic (Almeida et al. 1981), part of it consolidated as a product of a vast Neoproterozoic orogenic system associated with the assembly of Western Gondwana (e.g., Almeida et al. 1981; Brito Neves et al. 2000, 2014; Neves 2003; Santos et al. 2010; Ganade et al. 2014). Due to the diverse and complex geologic arrangements found in this province, some models have been proposed to explain its development, such as: (i) amalgamation of allochthonous/exotic terranes (Jardim de Sá et al. 1992; Santos 1995; Santos 1996; Santos and Medeiros 1999; Brito Neves et al. 2000, 2018, 2021); ii) Reworking of the Paleoproterozoic crust during an intracontinental/intracratonic Ediacaran orogeny (Neves 2015; Neves et al. 2021); iii) Different phases of a Wilson cycle that includes rifting, drifting, subduction and continent-continent collision (Caxito et al. 2014a, 2014b, 2016); iv) continent-continent collision on the northwestern margin and intracontinental reworking in the interior of the province, including destabilization of adjacent cratons in the form of ribbon continents (Ganade et al. 2014, 2016, 2021).

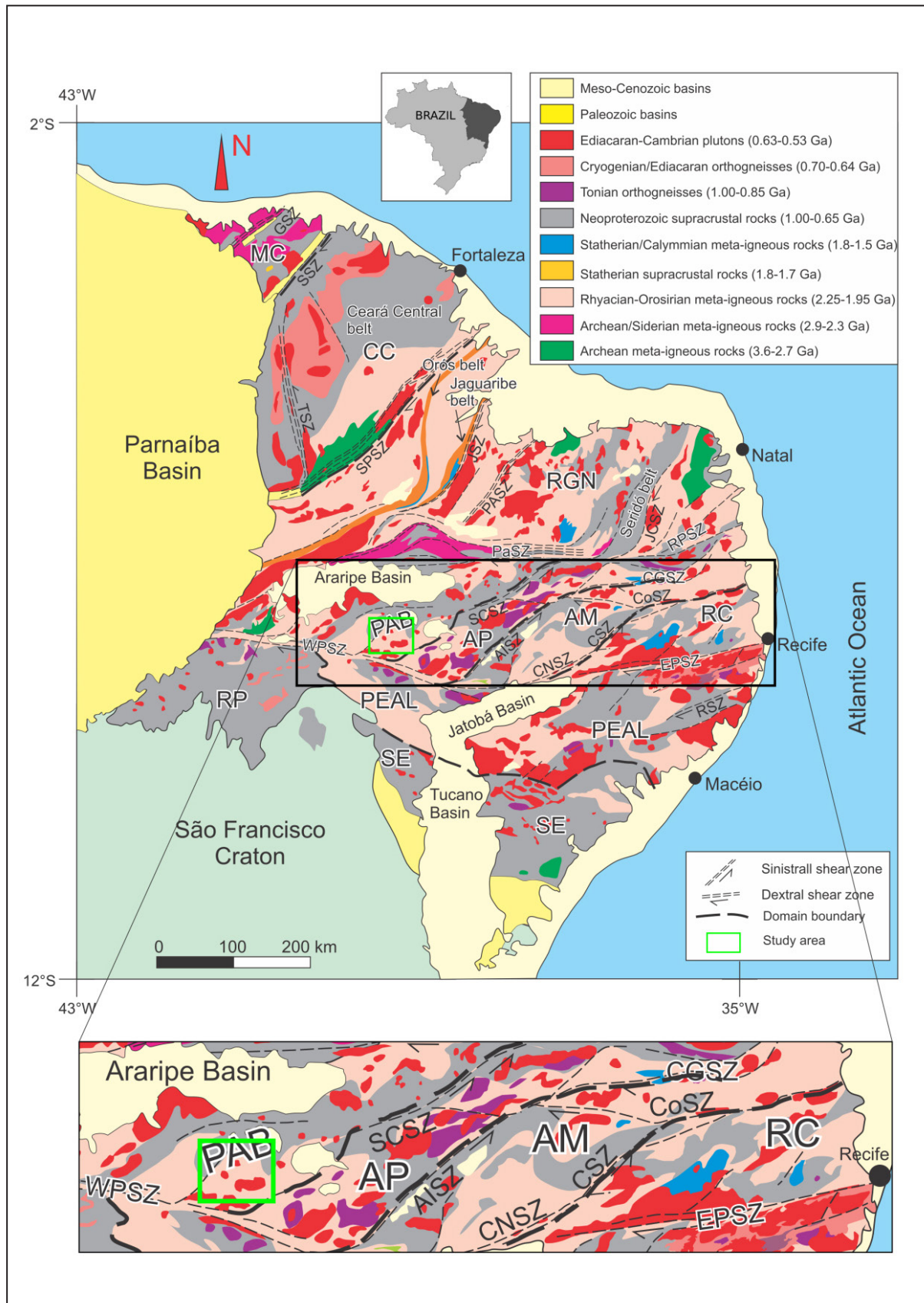
Based on prominent crustal discontinuities, Brito Neves et al. (2000) partitioned the province into several distinct domains: Médio Coreaú, Ceará Central, Rio Grande do Norte, Central or Transversal Zone, and Meridional. These domains are thought to record a polyphasic history of accretion and collision events, culminating in an intricate mosaic of tectonostratigraphic terranes. Analogous tectonic episodes are delineated in the African counterpart of the province, particularly within the Trans-Saharan Belt located between the Hoggar Shield and the Benin-Nigerian Province (Black et al. 1994; Liégeois et al. 1994; Liégeois et al. 2003). Gold deposits studied here are concentrated within the Central Domain, specifically in the Piancó-Alto Brígida domain.

The Central Domain, also known as the Transversal Zone, is a crustal structure characterized by a sigmoidal arrangement, bounded by two east-west-oriented shear zones: Patos to the north and Pernambuco to the south (Figure 1). The Central Domain (Transversal Zone) is characterized by a network of dextral strike-slip shear zones with E-W to ENE-WSW orientation and sinistral strike-slip shear zones with NNE-SSW to NE-SW orientation (Vauchez and Egydio-Silva 1992; Neves and Vauchez 1995; Vauchez et al. 1995; Neves and Mariano 1999; Neves et al. 2000; Silva and Mariano 2000; Archanjo and Fetter 2004; Archanjo et al. 2008; Hollanda et al. 2010) closely associated with significant Neoproterozoic magmatism.

The Central Domain has been further divided into tectonostratigraphic terranes (Figure 1), including the Piancó-Alto Brígida (PAB), Alto Pajeú (AP), Alto Moxotó (AM), Rio Capibaribe (RC) (Santos and Medeiros 1999; Brito Neves et al. 2000; Van Schmus et al. 2008), and sub-terrains such as Riacho Gravata and São José do Caiana (Santos et al. 2010; Brito Neves et al. 2005, 2016).

The PAB or the equivalent Cachoeirinha-Salgueiro Belt (Sial 1986; Sial and Ferreira 2016) originated through collision by accretion during the Cryogenian-Ediacaran transition (Brito Neves et al. 2018). The Piancó-Alto Brígida terrain comprises Paleoproterozoic basement rocks, Neoproterozoic supracrustal rocks with low- to medium-grade metamorphism belonging to the Cachoeirinha Group, as well as the Salgueiro Complex, and plutonic bodies from the Ediacaran period (Silva Filho 1984; Brito Neves et al. 1995; Caby et al. 2009).

The Cachoeirinha Group includes metapelites and metasandstones intercalated with acidic metavolcanic





rocks, iron formations, and metacarbonate rocks from the Santana dos Garrotes Formation. The Serra do Olha d'Água Formation comprises layers of metaconglomerates, immature sandstones, metagraywackes, and meta-rhyolites, which are exposed at the base of the Cachoeirinha Group (Medeiros 2004). The Salgueiro Complex is characterized by micaceous schists, quartzites, and, to a lesser extent, graphitic schists, ferruginous metacherts, and acidic to intermediate metavolcanic rocks (Silva Filho 1984).

The Neoproterozoic granitic plutonism in the Transversal Zone comprises three main events. The first event occurred between 650 and 600 Ma and is associated with plutons displaying a calc-alkaline signature, including high-K calc-alkaline and shoshonitic compositions (Guimarães et al. 2004; Ferreira et al. 2004). These bodies typically exhibit low-angle foliation and are either antecedent or contemporaneous with migmatization events and the metamorphic peak of the Transversal Zone/Central Domain (Guimarães et al. 2004; Neves et al. 2006).

The second event occurred between 590 and 570 Ma and is characterized by a voluminous magmatism that includes high-K calc-alkaline rocks associated with K-diorites, peralkaline to ultrapotassic potassic syenitoids (Ferreira et al. 2004), and high-K metaluminous syenitoids. This post-collisional magmatism records the transition from tangential tectonics to transcurrent/transpressive tectonics that developed in the province (Guimarães et al. 2004; Lages et al. 2016). The last event, which extended from 540 to 520 Ma, is associated with the emplacement of calc-alkaline plutons exhibiting signatures of A-type granites and peralkaline dikes, representing the post-orogenic phase (Guimarães et al. 2004).

The Serrita Suite formed plutonic stocks that crop out in the study area and are classified as peraluminous leucogranodiorite to leucotonalite with trondhjemitic characteristics (Sial 1986; Neves 1986). This classification is based on its petrographic characteristics, including magmatic epidotes, which exhibit more potassic features than true trondhjemitic, with a  $K_2O$  content greater than 2.5% (Sial and Ferreira 2016). Geochemically, the Serrita Stock is part of the magmatic epidote-bearing calc-alkaline and trondhjemitic plutons, indicating its formation in a magmatic arc setting (Sial and Ferreira 2016). The age of the Serrita Stock has been determined to be approximately 630 million years old (Sial and Ferreira 2016); however, the rounded ellipsoidal shapes of the bodies, with a northeast-trending axis and discrete brittle-ductile strike-slip shear zones, suggest a syn-kinematic setting younger than this supposed age.

The Serrita-Salgueiro District of the Cachoeira-Salgueiro-Gravatá Metallogenic Province (Beurlen 1995; Santos et al. 2014; Klein et al. 2024) comprises predominantly metasediments, granodiorites/tonalites, and quartz veins within the Salgueiro and Cachoeirinha schists, impacting the Serrita Intrusive Suite and Barra Verde Stock. Studies on Serrita gold deposits are interpreted as orogenic gold deposits due to hydrothermal alterations and low-salinity, aqueous-carbonic fluids, resulting in chloritization, carbonatization, and sericitization halos (Marinho and Gomes 2013; Beurlen et al. 1997). The ongoing interest in these areas is fueled by the high market value of gold and the potential for discovering new deposits, making them important targets for geological and metallogenic studies.

### 3. Analytical methods

In order to better characterize the studied mineralizations, two hundred fifty-five (255) gold particles from quartz veins distributed in the following occurrences along the Serrita-Salgueiro District: Santa Rosa (AL-010.vein, AL-010. boxwork), Sítio Algodões and Algodões Mine (AI-012, AI-013, GL-018), Barra Verde Mine and Santa locality (AL-011, CP-025.galena, chalcopyrite vein), and Garimpo do Gavião (AL-068), the material was crushed and concentrated in a pan. The gold particles obtained were investigated using Electron Microprobe Analysis (EPMA) to capture variations in gold composition. The chemical composition was analyzed using a JEOL JXA-8230 electron microprobe at the Electron Microprobe Laboratory of the State University of São Paulo. The analyses were conducted at an acceleration voltage of 25 kV, a beam current of 100 nA, and a beam diameter of 1-10  $\mu$ m. Calibration standards included natural and synthetic minerals from P&H Developments and Geller. The elements analyzed in EPMA and detection limits values are: Au (436 ppm), Ag (44 ppm), Hg (109 ppm), Pt (121 ppm), Cu (41 ppm), Ni (36 ppm), Co (33 ppm), As (55 ppm), Pb (93 ppm), S (28 ppm), Pd (9 ppm). Petrographic analyses of hydrothermally-altered granitoids and gold-mineralized quartz veins helped to understand the mineral assemblage associated with the Au and Au-Ag particles.

### 4. Geology of the Serrita-Salgueiro District

The Serrita-Salgueiro District (Beurlen 1995; Santos et al. 2014; Klein et al. 2024) comprises the contiguous Salgueiro and Serrita areas (Figure 2). The Salgueiro area encompasses the occurrences and mines in the Salgueiro and Verdejante municipalities, while the Serrita area includes the occurrences and mines of Serrita, Barra Verde, and Cedro.

#### 4.1 Salgueiro area

The Salgueiro area comprises the gold occurrences near Salgueiro, in Monte Alegre (Salgueiro), and Algodões (Verdejante) in the State of Pernambuco. These are recent discoveries made by artisanal miners. The Monte Alegre mining area is mainly associated with veins hosted in tonalites to granodiorites of the Serrita Suite, while the mineralizations in Algodões are hosted in metasediments (garnet mica-schists) of the Salgueiro Complex (Figure 3A).

The Salgueiro Complex consists of garnet mica schists and quartz-feldspathic metarhythmites with millimeter- to centimeter-scale micaceous and quartz bedding in the mining areas. The mineralogy includes biotite, muscovite, quartz, garnet, sillimanite, and cordierite, presenting an upper greenschist to amphibolite facies as a regional metamorphic gradient. Chlorite and carbonate are the most common hydrothermal alterations on these schists. The gold-mineralized quartz veins are massive and form tabular bodies (Figure 3B), sometimes with fragments of the host rocks. They exhibit an arborescent pattern in cross-sections and consist of milky quartz, with or without sulfides, carbonates (calcite in close contact with wall-rocks and siderite within quartz veins), hematite, limonite, and boxwork textures (partially filled with sulfides, hematite/goethite, and clay minerals) related to the ore (Figure 3C). The contact with the host rocks is abrupt



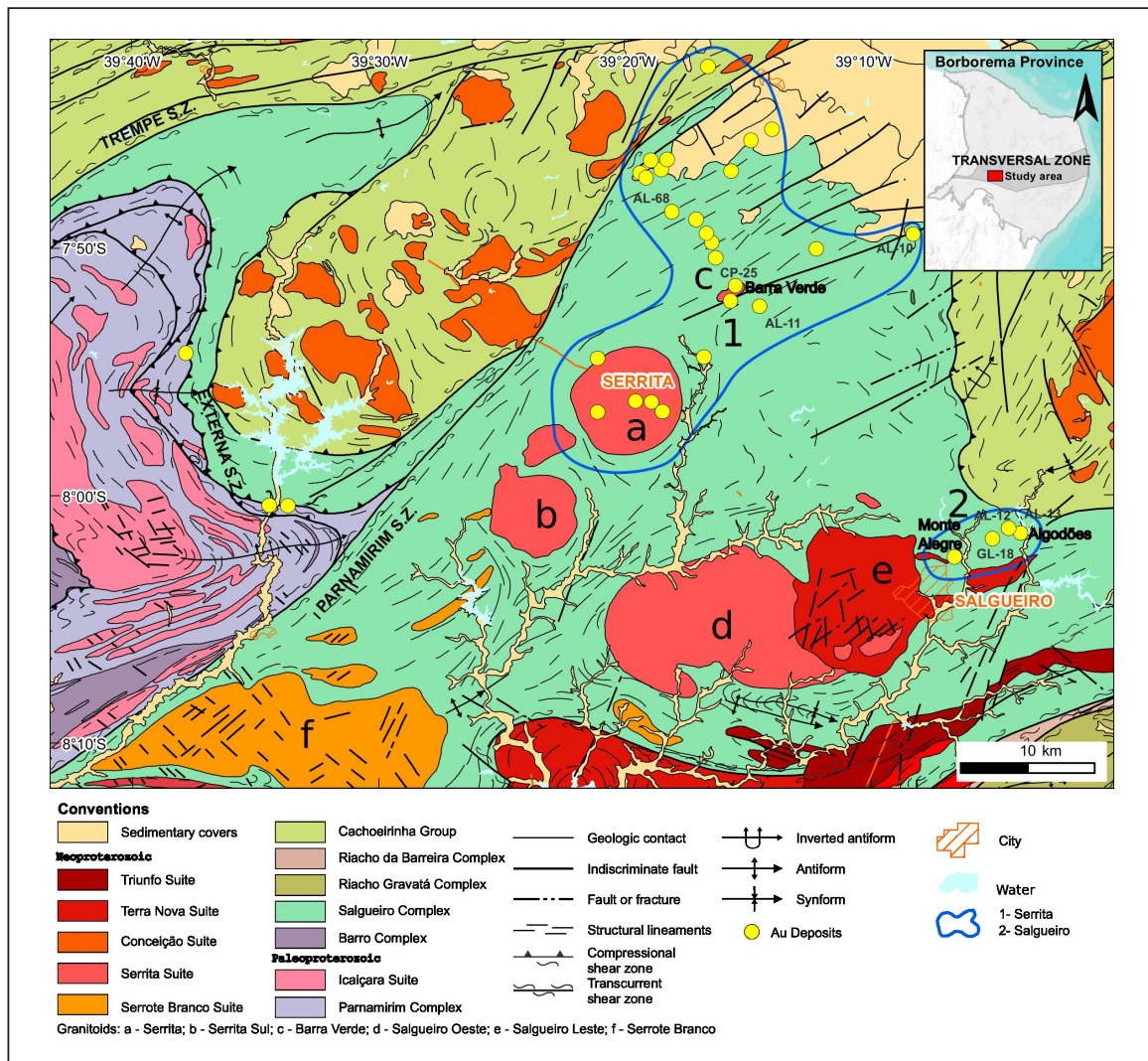


FIGURE 2. Geological map of the study area with the main gold occurrences and location of the Serrita (1) and Salgueiro (2) areas of the Serrita-Salgueiro District. Modified after Santos et al. (2021).

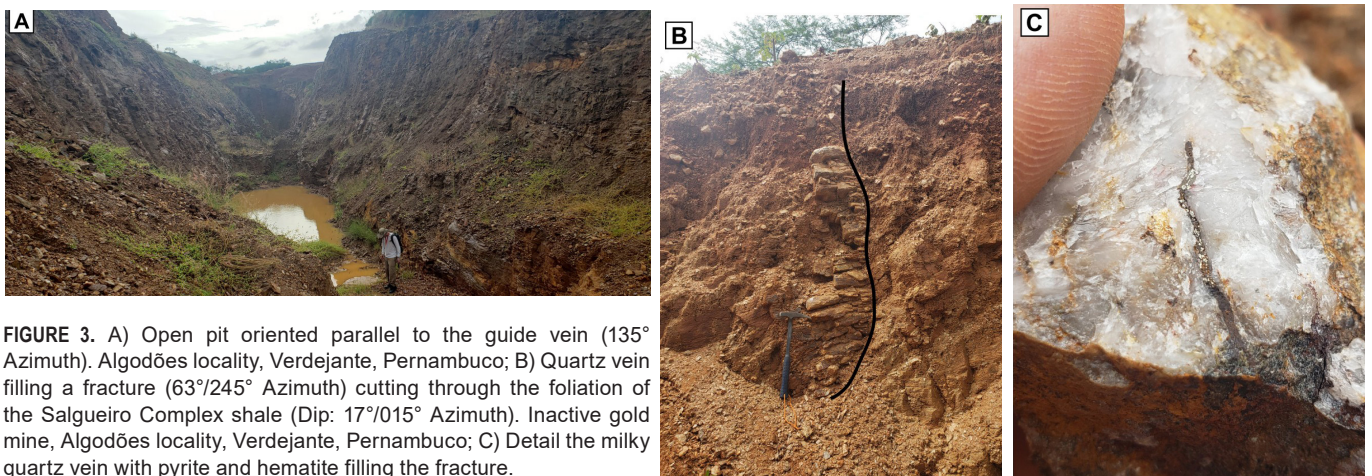


FIGURE 3. A) Open pit oriented parallel to the guide vein (135° Azimuth). Algodões locality, Verdejante, Pernambuco; B) Quartz vein filling a fracture (63°/245° Azimuth) cutting through the foliation of the Salgueiro Complex shale (Dip: 17°/015° Azimuth). Inactive gold mine, Algodões locality, Verdejante, Pernambuco; C) Detail the milky quartz vein with pyrite and hematite filling the fracture.

(Figure 3B), and the veins range from 10 to 50 cm in width, positioned vertically to subvertically, with E-W, NE-SW, and NNW-SSW orientations similar to what is observed in the Serrita outcrops. Sometimes, a thick, milky quartz central vein is used as a guide vein to prospect mineralized veins and is oriented NW-SE.

Under the microscope, gold particles occur within quartz grains both as unencapsulated “free” gold and as gold associated with cavities (possibly remnants of inclusion-hosted sulfides), as seen in Figures 4A and 4B. Gold can also occur with hematite in fractures. Pyrite occurs freely in quartz veins and/or filling fractures, with a pale yellow color and occasional



fracturing (Figures 4C and 4D). Chalcopyrite and arsenopyrite are other sulfide phases of the mineralization, occurring in contact or as inclusions, mainly in pyrite. In addition to these minerals, martite, hematite, and siderite occur, filling fractures (Figure 4D). It is worth noting the presence of smoky to milky quartz veins parallel to the foliation of the host schist, often boudinaged, with cavities and, locally, associated with sulfides such as pyrite.

#### 4.2 Serrita area

The Serrita area encompasses the gold occurrences located to the north-northeast of the town of Serrita, in Pernambuco. The Serrita-type granites include biotite-hornblende monzodiorite, monzonite, quartz monzonite, tonalites, and biotite granite. They are considered late orogenic, with trondhjemitic affinity (Sial 1986; Neves 1986, 1988; Kosin et al. 2004) (Figure 2).

In the Serrita area, there is the Barra Verde mining area, where lithotypes consist of fine- to medium-grained equigranular leucogranodiorites to leucotonalites, composed of plagioclase, microcline, quartz, biotite, and amphibole (Figures 5A and 5B). The plagioclase crystals exhibit albite and pericline twinning, substituting muscovite and sericite, indicating sericitization. Biotite shows yellow to greenish-yellow pleochroism and alters to muscovite, chlorite, and epidote. Accessory minerals include titanite, zircon, and apatite.

Hydrothermal alteration intensifies toward the vein walls. Distal margins display fine-grained white mica with trace fluorite (Figures 5F, 6C). Where the vein network is denser, centimeter-scale replacement of plagioclase and biotite by K-feldspar, muscovite, and sericite is common, locally with K-feldspar flooding and perthitic textures at the granite–vein contact (Figures 5B–C, 6B). Away from veins, feldspars, mainly plagioclase, remain better preserved and muscovite is scarce (Figure 6A). In proximal thin sections, secondary muscovite increases and quartz is recrystallized; representative modal estimates reach ~45% white mica and ~35% quartz, with ~9% microcline, ~6% plagioclase, and ~1% epidote.

Within the vein system, milky to sub-translucent quartz veins form one to two anastomosing sets and attain widths of ~1–1.5 m. Coarse muscovite occurs at vein contacts where plagioclase is replaced by muscovite, outlining centimeter-scale alteration bands (Figures 5B, 6B–C). Galena is frequent as fracture-fill and as centimeter-scale aggregates encapsulated by quartz; pyrite and chalcopyrite also occur within the vein sets (Figures 5D–E, 6D).

There are two types of sub-vertical mineralized veins and one thick, commonly barren, central vein according to the temporal order: 1) large NW-oriented, commonly barren veins (central vein); 2) highly fractured quartz veins with ENE-ESE orientation, which have the highest content in Au, Ag, and Pb; 3) late N-S/NNW-SSE-oriented veins.

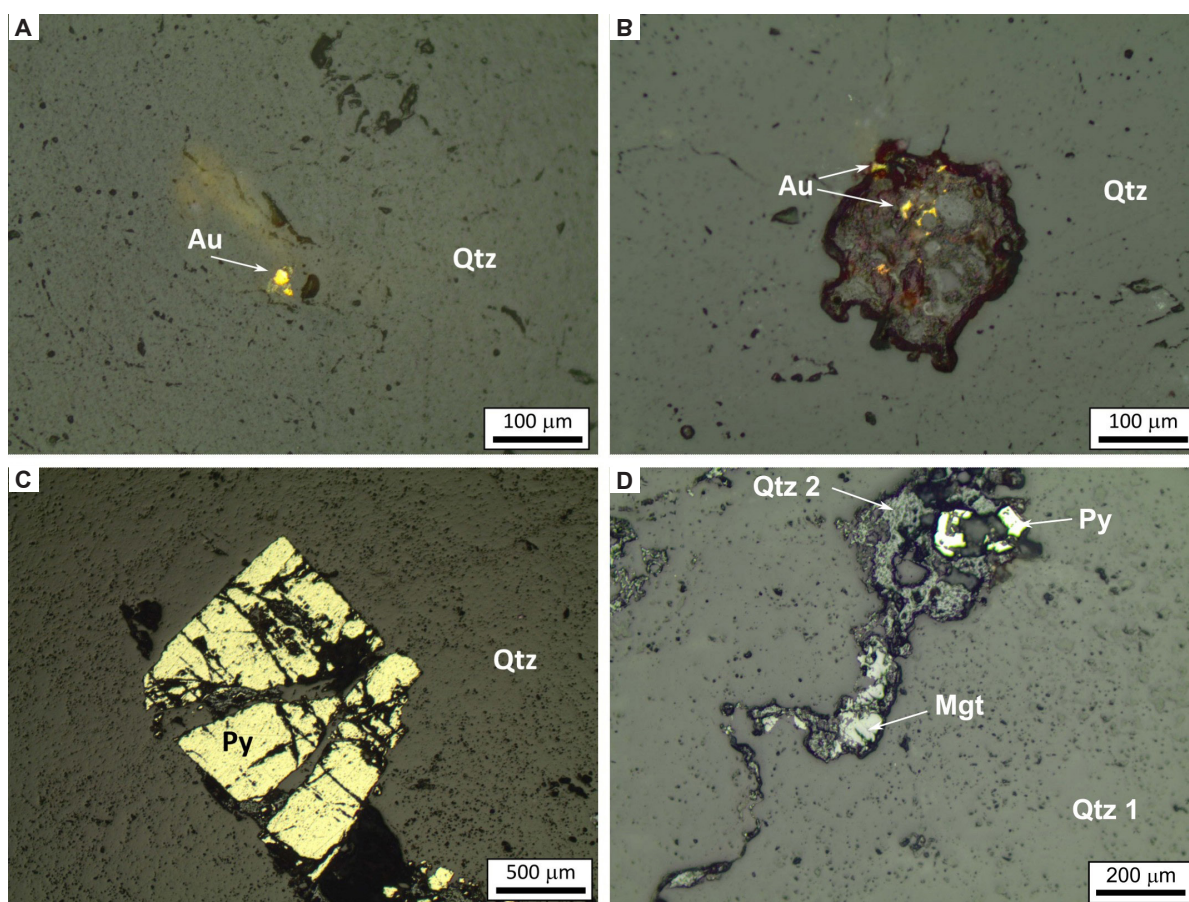


**FIGURE 4.** Mineralized quartz vein under the microscope (polished section), Algodões Mine. A) Free gold (Au) grain in quartz vein (Qtz), sample AL-082; B) Primary Gold (Au) present in cavity, possibly hosted as inclusion within sulfide now decomposed, sample AL-082; C) Fractured euhedral pyrite (Py) crystal included in quartz (Qtz), sample CP-145A; D) Fracture in quartz vein (Qtz) filled with silica (Qtz2), magnetite/spinel (Mgt), and pyrite (Py), sample CP-145A.



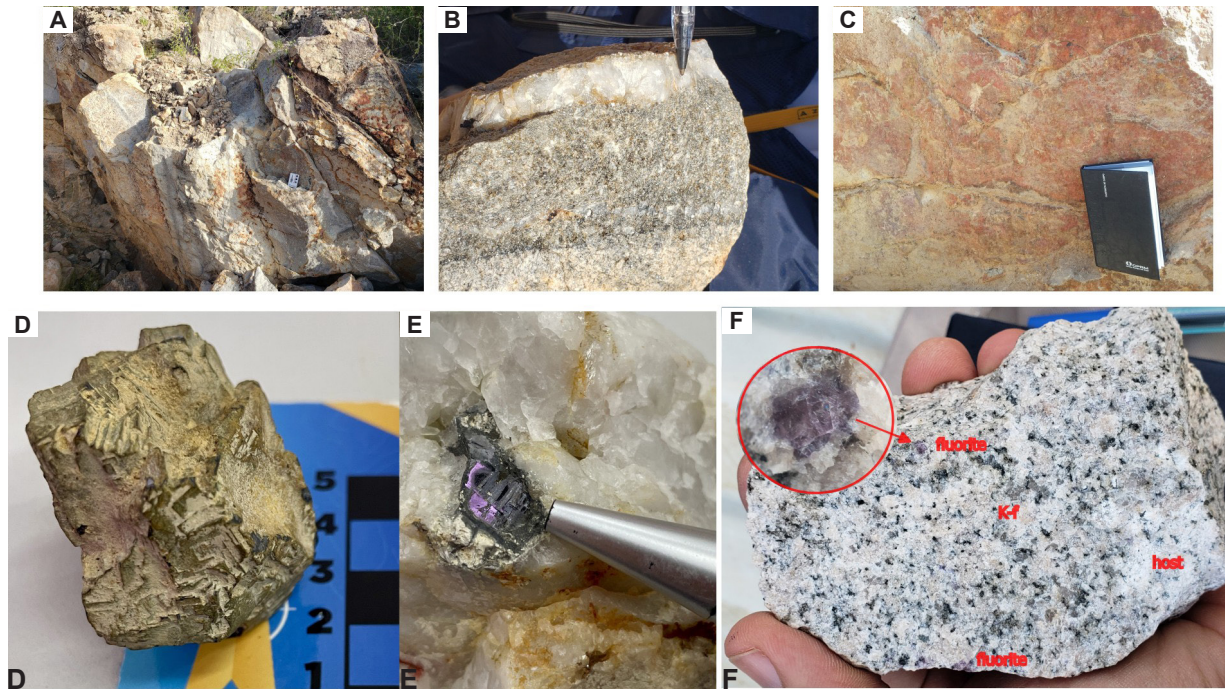


**FIGURE 5.** A) Overview of the Serrita Suite tonalite closer to the quartz veins; B) Detail of the coarse muscovite hydrothermal halo in contact with the quartz vein; C) Field appearance of the leucogranodiorite with potassic to phyllic alteration halo; D and E) Centimetric galenas formed during sulfide stage and encapsulated by quartz vein; F) Presence of fluorite in host tonalite rock composition. Barra Verde Gold artisanal Mine, Serrita, Pernambuco State.

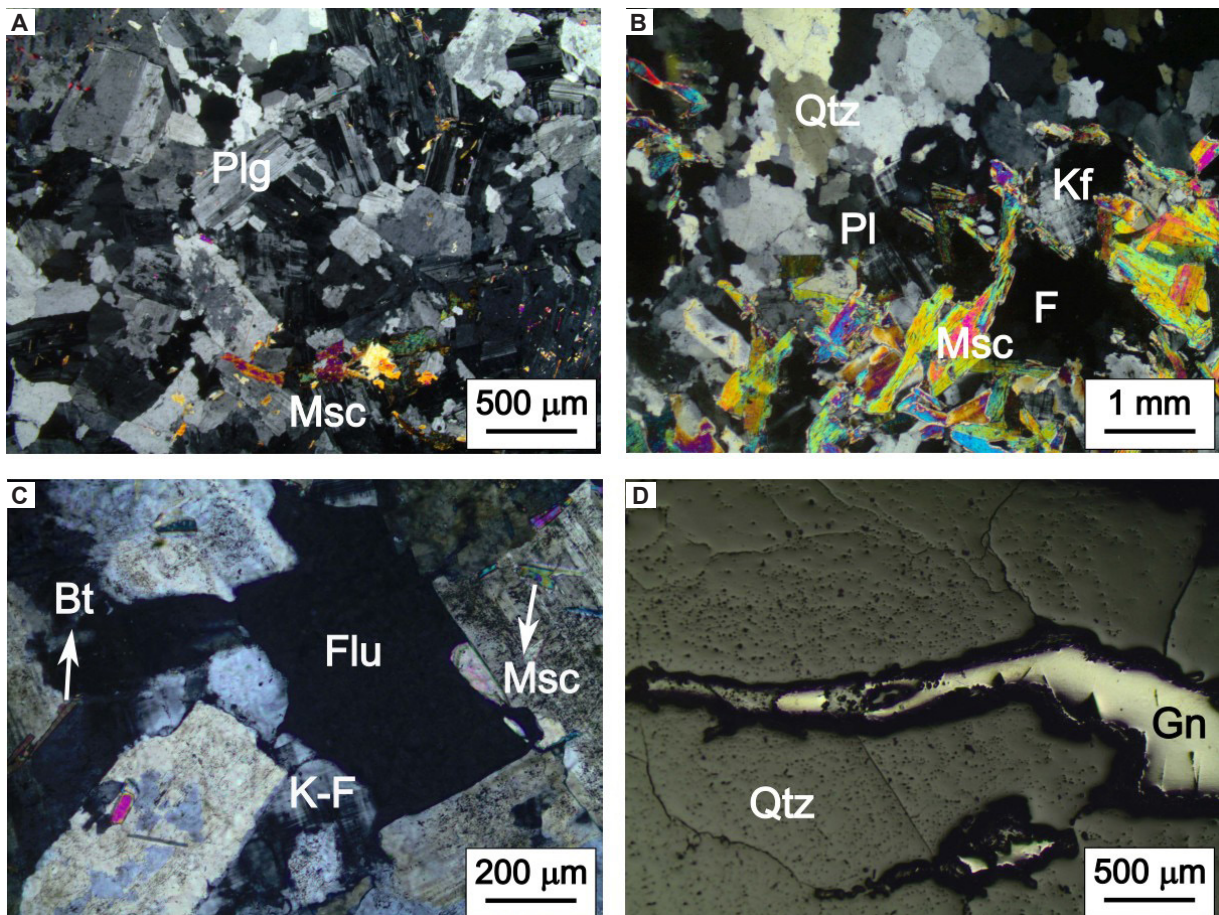


**FIGURE 6.** Photomicrographs of the Serrita Suite tonalite. A) Well-preserved rock with numerous plagioclase (Plg) crystals and almost absence of muscovite (Msc) and; B) Rock intersected by a quartz vein (Qtz); in this proximal halo, plagioclase has mainly been replaced by Kfeldspar + muscovite (Msc), highlighting the hydrothermal potassic to phyllic halo to the rock; C) Idiomorphic Fluorite in low hydrothermalized granitic portion; D) Galena (Gn) filling fractures in a quartz vein (Qtz). Barra Verde Gold Mine, Serrita, Pernambuco.



In this area, the guiding veins that control mineralization predominantly trend NW-SE (115° Az), perpendicular to the regional foliation trend. The mineralized quartz veins within the granites tend to be coarser than in schists and present as sheeted veins. Sub-vertical sets exhibit mainly NW-SE directions; meanwhile, the directions 1, 2, and 3 presented above are expected to be similar to those in the schists.

## 5. Mineral chemistry

Electron microprobe analyses to capture variations in gold composition were conducted on 100 gold particles from Salgueiro and 139 gold particles from Serrita mineralizations of Serrita-Salgueiro District: quartz veins in Salgueiro area - Sítio Algodões (AL-012, AL-013) and Algodões Mine (GL-018) and Serrita area - Santa Rosa (AL-010), Barra Verde Mine and Santa Cruz locality (AL-011, CP-025) and Garimpo do Gavião (AL-068). The macroscopic features of quartz veins are listed in Table 1.

The total closure of gold particle analyses considered for this study ranges from 95% wt.% to 101% wt.%, combining the highest possible amount of data, containing 90% of the analyses, with the fact that other elements such as Bi, Te, and Sb, among others, were not analyzed, which may be present in

gold particles as minor or trace elements. The main statistical values of mineral chemistry are summarized in Table 2.

Gold particles from Serrita area mineralizations exhibit Au and Ag contents ranging from 74 to 92 wt.% and 6.1 to 22 wt.%, respectively. Salgueiro area gold particles exhibit Au and Ag contents ranging from 44 to 93 wt.% and 6.9 to 52 wt.%, respectively (Table 1). The gold fineness, which measures the gold purity, expressed by the formula  $[Au / (Au + Ag) \times 1000]$ , varies from 770 to 938 in the Serrita area and ranges from 461 to 930 in the Salgueiro area.

The elements Hg, Ni, Co, Pb, and S concentrations show low values above the detection limit of the EPMA, evidenced in boxplot diagrams, and exhibit a scattered distribution vs. Au, except for Hg, whereas Cu, As, Pt, and Pd concentrations have a value of zero (Figure 7, Figure 8, Table 2). The elements Au, Ag, and Hg show notable correlations, highlighting the compositional differences in gold between each area. When each location is plotted separately on binary diagrams (Figure 9), the values reveal a strong negative linear correlation between Au and Ag for all gold particles in the Serrita-Salgueiro District, a positive linear correlation between Au and Hg, and a negative correlation between Ag and Hg for a few areas, mainly for Algodões Mine, Barra Verde, and Santa Cruz localities (Figure 10).

TABLE 1: Macroscopic features of the studied veins in the Serrita-Salgueiro district.

Sample	Locality	Exposure style	Host-rock	Assemblage	Width/length	Direction	Textures	Wall-rock
AL-10	Santa Rosa	trench; shaft along veins	dense milk quartz veins	pyrite, chalcopryrite	Two shafts measuring 1.5x1.5x1 m	Veins 34/109	boxworks with limonite	biotite schist
AL-10-boxwork	Santa Rosa	trench; shaft along veins	dense milk quartz veins	pyrite, chalcopryrite, oxides	Shafts measuring 2x1.5x1 m	Veins 34/110	boxworks with limonite	biotite schist
AL-11	Barra Verde / Santa Cruz	trench; shaft along veins	milk quartz veins	pyrite, oxides	30m length	N315; vertical	boxworks	biotite schist
AL-12	Sítio Algodões	trench; shaft along veins	milk quartz veins	pyrite, chalcopryrite	20m length	N145; vertical	boxworks with oxidized material; breccia/stockwork net vein	biotite schist
AL-13	Sítio Algodões	trench; shaft along veins	milk quartz veins		50m length	N15; subvertical	boxworks with limonite	biotite schist
AL-68	Garimpo do Gavião	shaft	dense milk quartz veins	coarse free Au, secondary limonite and clay	400m extension	Pit N25E with N80W 'veinlets'	boxworks with clay, limonite	cordierite-garnet schist/paragneiss
CP-25	Barra Verde	trench; shaft along veins	milk quartz veins	arsenopyrite, galena, covellite	parallel veins with up to 200m extension	veins with sulphide N6E; and 240/43 metasomatic halos bounding quartz veins	Potassification, sericitic alteration, sulphides	fine-grained leuco tonalite
GL-18	Algodões Mine	trench	milk quartz veins	pyrite, oxides, clay halo	2-3m width	N30W; vertical	boxworks with clay and oxidized material; breccia/stockwork net vein; chlorite halo in contact with schist	cordierite-garnet schist/paragneiss

TABLE 2: Results of chemical analyses on goDL grains from the Serrita and Salgueiro localities.

	Locality	N° GoDL Particles	Min	1° Quartile	Mean	Median	3° Quartile	Max
Au	(Salgueiro) Sítio Algodões	17	78	83	85	86	87	89
	(Salgueiro) Algodões Mine	83	44	51	61	56	69	93
	(Serrita) Santa Rosa	24	87	90	90	90	91	92
	(Serrita) Santa Cruz	11	83	85	88	90	91	92
	(Serrita) Garimpo do Gavião	89	82	85	86	86	88	90
	(Serrita) Barra Verde	15	74	80	82	82	86	87
Ag	(Salgueiro) Sítio Algodões	17	8.5	10	12	12	14	18
	(Salgueiro) Algodões Mine	83	6.9	27	35	39	45	52
	(Serrita) Santa Rosa	24	6.8	7.6	8	7.7	8.4	9.6
	(Serrita) Santa Cruz	11	6.1	7.7	10	9	12	16
	(Serrita) Garimpo do Gavião	89	8.5	10	12	12	13	15
	(Serrita) Barra Verde	15	11	13	15	15	17	22
Finesses	(Salgueiro) Sítio Algodões	17	815	859	874	882	896	913
	(Salgueiro) Algodões Mine	83	461	530	633	588	718	931
	(Serrita) Santa Rosa	24	902	914	919	921	922	931
	(Serrita) Santa Cruz	11	834	873	896	909	922	938
	(Serrita) Garimpo do Gavião	89	842	867	880	874	894	914
	(Serrita) Barra Verde	15	770	827	842	843	871	886
Hg	(Salgueiro) Sítio Algodões	17	0.25	0.26	0.28	0.27	0.29	0.33
	(Salgueiro) Algodões Mine	83	0.076	0.12	0.16	0.15	0.19	0.25
	(Serrita) Santa Rosa	24	0.3	0.33	0.34	0.34	0.34	0.38
	(Serrita) Santa Cruz	11	0.29	0.31	0.33	0.33	0.34	0.36
	(Serrita) Garimpo do Gavião	89	0.24	0.29	0.31	0.31	0.34	0.39
	(Serrita) Barra Verde	15	0.24	0.24	0.27	0.27	0.28	0.31
Pb	(Salgueiro) Sítio Algodões	17	<DL	<DL	0.011	0.0079	0.022	0.033
	(Salgueiro) Algodões Mine	83	<DL	0.0046	0.016	0.013	0.024	0.051
	(Serrita) Santa Rosa	24	<DL	0.011	0.018	0.016	0.024	0.045
	(Serrita) Santa Cruz	11	<DL	0.004	0.016	0.011	0.024	0.049
	(Serrita) Garimpo do Gavião	89	<DL	0.0017	0.016	0.015	0.025	0.077
	(Serrita) Barra Verde	15	<DL	0.0051	0.015	0.01	0.023	0.04
S	(Salgueiro) Sítio Algodões	17	<DL	0.0007	0.0045	0.0036	0.0071	0.021
	(Salgueiro) Algodões Mine	83	<DL	0.0041	0.006	0.0055	0.008	0.017
	(Serrita) Santa Rosa	24	0.0032	0.0064	0.009	0.0093	0.013	0.013
	(Serrita) Santa Cruz	11	0.0018	0.0061	0.0093	0.0084	0.011	0.024
	(Serrita) Garimpo do Gavião	89	<DL	0.0033	0.01	0.0084	0.014	0.049
	(Serrita) Barra Verde	15	<DL	0.0021	0.0059	0.0052	0.0092	0.015
Cu	(Salgueiro) Sítio Algodões	17	<DL	<DL	0.00041	<DL	<DL	0.0069
	(Salgueiro) Algodões Mine	83	<DL	<DL	<DL	<DL	<DL	<DL
	(Serrita) Santa Rosa	24	<DL	<DL	<DL	<DL	<DL	<DL
	(Serrita) Santa Cruz	11	<DL	<DL	<DL	<DL	<DL	<DL
	(Serrita) Garimpo do Gavião	89	<DL	<DL	<DL	<DL	<DL	<DL
	(Serrita) Barra Verde	15	<DL	<DL	<DL	<DL	<DL	<DL
Ni	(Salgueiro) Sítio Algodões	17	<DL	<DL	0.000041	<DL	<DL	0.0004
	(Salgueiro) Algodões Mine	83	<DL	<DL	0.0001	<DL	<DL	0.0025
	(Serrita) Santa Rosa	24	<DL	<DL	0.00043	<DL	0.00083	0.0032
	(Serrita) Santa Cruz	11	<DL	<DL	<DL	<DL	<DL	<DL
	(Serrita) Garimpo do Gavião	89	<DL	<DL	0.00016	<DL	<DL	0.0031
	(Serrita) Barra Verde	15	<DL	<DL	<DL	<DL	<DL	<DL
Co	(Salgueiro) Sítio Algodões	17	<DL	0.0009	0.0022	0.0023	0.0038	0.0058
	(Salgueiro) Algodões Mine	83	<DL	<DL	0.001	0.0004	0.0017	0.0054
	(Serrita) Santa Rosa	24	<DL	0.001	0.0022	0.0021	0.0033	0.0052
	(Serrita) Santa Cruz	11	<DL	0.00055	0.0022	0.0024	0.0033	0.0051
	(Serrita) Garimpo do Gavião	89	<DL	0.0006	0.0018	0.0017	0.0027	0.0065
	(Serrita) Barra Verde	15	<DL	0.0002	0.0017	0.0014	0.0026	0.0047

&lt;DL: below detection limit

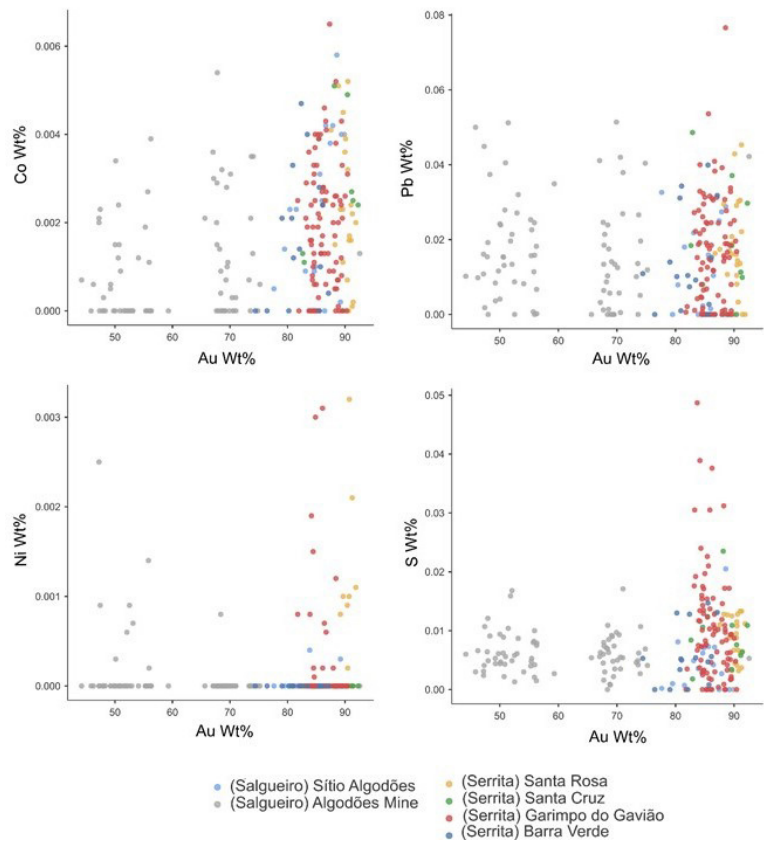


FIGURE 7. Diagrams of chemical composition for Co, Pb, Ni, and S vs Au of gold particles from the Serrita and Salgueiro localities.

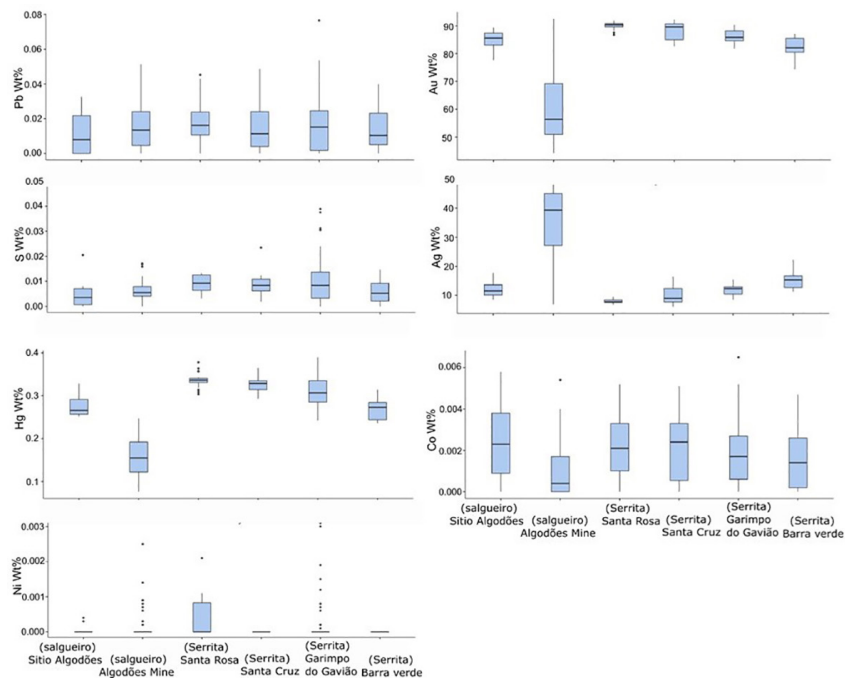
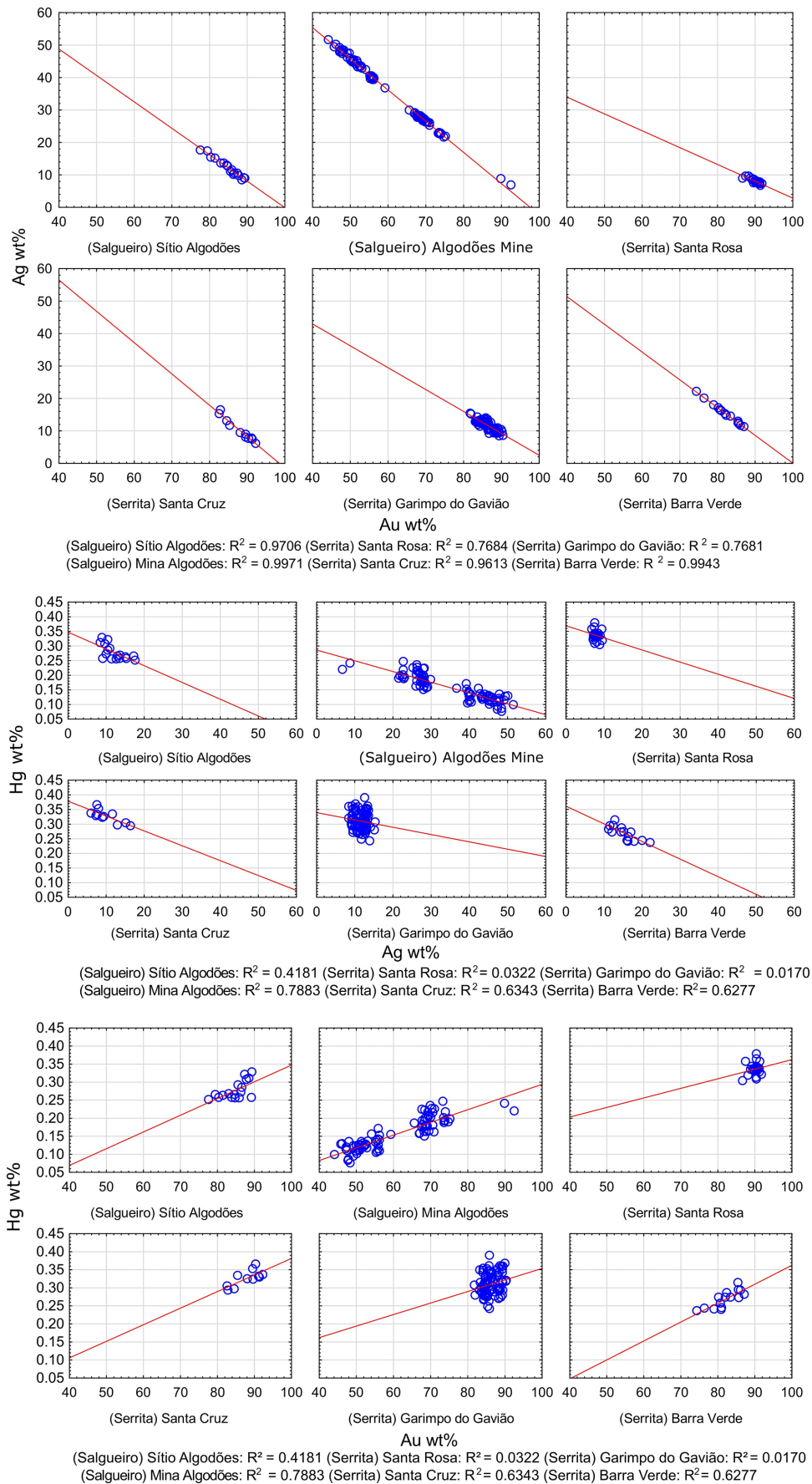


FIGURE 8. Boxplot diagrams of chemical analyses of gold from Serrita and Salgueiro localities.





**FIGURE 9.** DD diagrams of chemical composition for Au, Ag, and Hg of gold particles from the Serrita and Salgueiro localities.

## 6. Discussions

The investigation of gold particle composition has significantly contributed to primary mineralization studies (Chapman et al. 2021; Townley et al. 2003; Palacios et al. 2001). Additionally, the variation in the composition of gold particles is a source of information that can indicate the type of deposit source (Chapman et al. 2021).

The chemical compositions of gold particles from the studied area exhibit considerable similarity; however, notable differences emerge when examining specific localities within the collection. In all localities except Algodões Mine, Ag concentration ranges between 6.1 and 22 wt%, with Santa Rosa showing the lowest Ag concentrations, between 6.1 and 9.6 wt%. Additionally, a robust correlation is observed between Au and Ag across samples. In contrast, Au-Hg and Ag-Hg correlations are not uniformly present in gold particles across localities. Specifically, Sítio Algodões, Santa Cruz, and Barra Verde exhibit clear correlations among these elements, while Santa Rosa and Garimpo do Gavião do not display such patterns.

Algodões Mine is particularly distinct regarding Ag concentration variability in its gold particles, showing significantly higher Ag content than other sites. The gold grains from this locality can be categorized into two groups: one with exceptionally high Ag concentrations (52–40 wt%) and another with high concentrations (30–20 wt%). Two gold particles exhibit Ag concentrations below 10%, suggesting either the reduction of Ag content via supergene processes in near-surface environments, which altered gold composition (Hough et al. 2009), or the existence of a rarer, third group with low Ag concentrations. Another distinctive feature of Algodões Mine is the positive correlation between Au and Hg, also observed in Sítio Algodões, Santa Cruz, and Barra Verde.

The chemical variations in gold from the Serrita-Salgueiro District enable differentiation of mineralization groups based on the presence or absence of Au-Ag-Hg correlations and ranges of Ag concentration in gold particles. These distinctions become clearer when using gold fineness as an indicator, facilitating inferences on primary deposit style (Morrison et al. 1991; Liu and Beaudoin 2021; Ketchaya et al. 2022). This approach suggests that mineralization in the Serrita-Salgueiro District forms a hybrid system, incorporating an epithermal component at Algodões Mine along with probable contributions from orogenic, porphyry, and/or Reduced Intrusion-Related Gold (RIRG) systems (Figure 10).

Another means of assessing gold particle composition is through the Au-Ag-Cu ternary diagram, which serves as an indicator of the primary deposit style for gold mineralization (Townley et al. 2003; Omang et al. 2015; Ateh et al. 2021). Within the Serrita-Salgueiro District, gold particles fall within ranges consistent with hydrothermal, epithermal, and gold-rich porphyry deposits (Figure 11). Note that Cu contents are extremely low in most grains, causing points to cluster along the Au-Ag axis; consequently, the discriminatory power of this diagram is limited and should be treated as qualitative. Where Cu is above the detection limit, Serrita grains tend to show slightly higher Cu grades relative to Salgueiro, which is more consistent with an intrusion-related signature, whereas the Ag-rich compositions at Salgueiro are compatible with shallow epizonal/orogenic and/or epithermal conditions.

Overall, orogenic gold deposits and Reduced Intrusion-Related Gold Systems (RIRGS) share several similarities, suggesting that there may be overlap in their formation processes and fluid sources. Orogenic and RIRGS gold deposits are associated with ore-forming fluids, typically H<sub>2</sub>O-NaCl-CO<sub>2</sub>-rich, with low-to-moderate salinity. These fluids may also contain W, Te, and Bi elements, indicating a sulfide-dominated fluid source. Both deposit types exhibit similar mineralization styles, with auriferous sheeted vein arrays (Goldfarb and Groves 2015).

The gold mineralizations in the Serrita-Salgueiro District are hosted in quartz veins within metasediments of the Salgueiro Complex and granites of the Serrita Suite, arranged in fracture systems and faults of extensional systems, sheeted veins, and hydrothermal breccias with veins ranging from 0.1 to 1 meter in thickness, usually discordant (high angle) to the foliation of the host rock. These quartz veins, when mineralized, contain higher gold content and sulfides and constitute a complex stockwork of anastomosed vein systems originating from a central vein. In the field, these veins exhibit textural characteristics, such as boxworks or cavities (locally referred to as carious veins), which result from the leaching of sulfide phases. These veins occur extensively in the same direction and can reach up to 670 meters in the study area. In addition to the discordant veins, there are smoky to milky quartz veins concordant to the main foliation of the metasediments of the Salgueiro Complex. These veins have

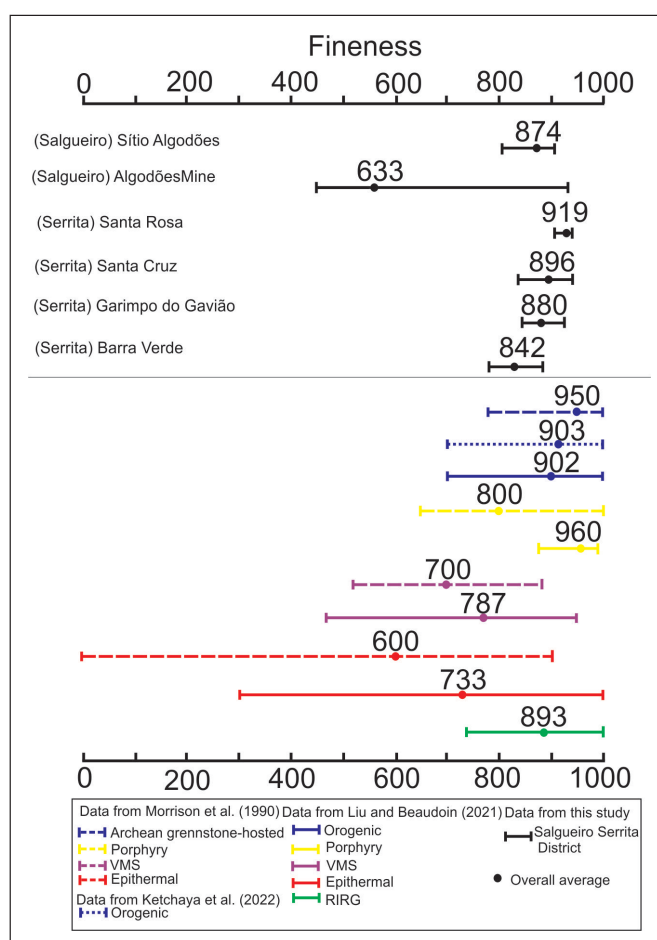
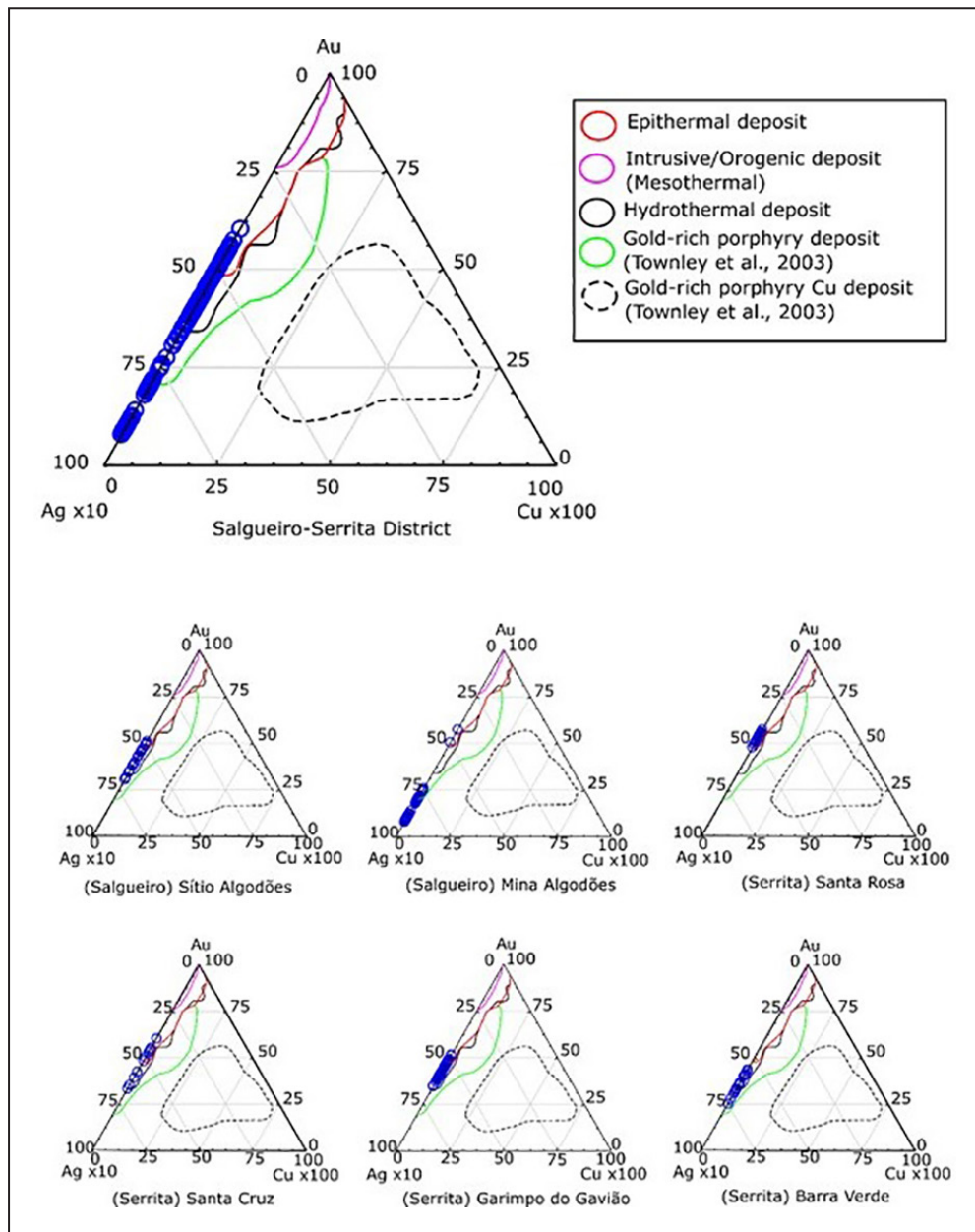


FIGURE 10. Comparative diagram of fineness values from the Serrita-Salgueiro district.



**FIGURE 11.** Ternary composition of native gold (Au–Ag–Cu) from the Serrita–Salgueiro district with Serrita grains tend to show slightly higher Cu relative to Salgueiro, consistent with a more intrusion-related signature, whereas Ag-rich compositions at Salgueiro are compatible with shallow epizonal/orogenic–epithermal conditions.

sulfide portions and may be related to mineralization in a minor proportion compared to discordant veins.

The distinction between free gold and sulfide-hosted gold highlights different precipitation mechanisms within these complex systems (Groves et al. 2003). Free gold is typically associated with orogenic systems, where it precipitates from  $\text{CO}_2$ -rich metamorphic fluids into quartz veins, whereas inclusion-hosted gold, especially within pyrite and chalcopyrite, tends to indicate precipitation from magmatic-hydrothermal fluids. In the Serrita–Salgueiro gold district, *free gold* is observed as visible native gold within quartz veins or otherwise outside sulfide minerals, in contrast to gold sequestered as inclusions within sulfides such as pyrite, arsenopyrite, and chalcopyrite; this dual mode of occurrence implies multiple mineralization processes and supports a hybrid genetic model

(with contributions from both metamorphic–orogenic and magmatic–hydrothermal gold-forming systems) for the deposit.

The chemical signatures of gold differ between the studied districts. Gold particles from the Serrita district have the highest gold content (fineness), while in the Salgueiro district, there are also significant concentrations of silver, nickel, cobalt, mercury, lead, and sulfur. This compositional difference reflects the sulfide paragenesis, with the Au–Pb–(Cu) association in Serrita and the Au–Ag–(As) association in Salgueiro.

Mercury isotopic compositions suggest a significant contribution from magmatic sources in iron oxide-copper-gold (IOCG) hydrothermal systems (Yin et al. 2023), and the recycling of Hg into volcanic-arc environments, where epithermal gold deposits are common, also highlights the



contribution of magmatic-hydrothermal processes to Hg enrichment in gold systems (Deng et al. 2021).

The isochores for the aqueous-carbonic primary and pseudo-secondary fluid inclusions from the Serrita area indicated entrapment pressures between 1.3 and 1.8 kbar (Beurlen et al. 1997), suggesting a shallower entrapment level, where, in low-pressure settings, mercury remains stable and is more likely to be trapped within the gold particles (Naumov et al. 2018). Elevated Hg in gold from the Serrita-Salgueiro district is consistent with shallow entrapment and magmatic-hydrothermal input, but we treat it as indicative rather than diagnostic, pending corroboration by fluid-inclusion data and paragenetic constraints.

Typical fluids in orogenic gold deposits encompass a range of compositions (Ridley and Diamond 2000; Goldfarb and Groves 2015; Groves et al. 2018). Aqueous-carbonic inclusions of low salinity and low molecular CO<sub>2</sub> content mainly represent mineralizing fluids.

Beurlen et al. (1997) investigated the fluid compositions in gold- and sulfide-mineralized quartz veins and barren quartz veins from the Barra Verde prospect, hosted in granodiorites and schists in the Serrita area. These authors described two fluid inclusion types: (FI-A) represented by primary and pseudo-secondary fluid inclusions, triphasic with aqueous-carbonic composition (H<sub>2</sub>O liq + CO<sub>2</sub> liq + CO<sub>2</sub> gas) at room temperature, and (FI-B) secondary fluid inclusions, aqueous bifasic (H<sub>2</sub>O liq + H<sub>2</sub>O gas) and aqueous monofasic (H<sub>2</sub>O liq).

Microthermometric data obtained for FI-A type revealed CO<sub>2</sub> melting temperatures of -56.6 to -59.3 °C (indicating contributions of CH<sub>4</sub> or N<sub>2</sub>), clathrate melting temperatures around 5.0 to 7.6 °C, ice melting temperatures of -4.3 to -0.5 °C, indicating low salinity of approximately 6.9% NaCl eq. Total homogenization temperatures for FI-A type ranged from 280 °C to 440 °C, with a concentration of around 341 °C, and for FI-B type, from 110 °C to 330 °C, with a concentration of around 320 °C (Beurlen et al. 1997). Additionally, Beurlen et al. (1997) suggested that these two immiscible fluids coexisted during alteration, quartz crystallization, deformation, and mineralization at temperatures ranging from 290 °C to 310 °C, characteristics similar to those found in other Archean metamorphic gold vein deposits.

The hydrothermal halo in RIRGS, identifiable by its zoned mineral associations of proximal Au-W-As and distal Ag-Pb-Zn metal assemblages, reflects the temperature of the fluids during mineral deposition and their interactions with surrounding rock formations (Groves et al. 2003; Hart 2007). These halos, commonly associated with magmatic fluids, exhibit a distinct spatial, temporal, and geochemical correlation with single intrusions (Sillitoe and Thompson 1998). They emerge within the hydrothermally-influenced area, encompassing the causative pluton and a variety of mineral deposit types, including skarns, replacements, and veins (Hart 2007).

On the other hand, orogenic gold systems present hydrothermal architectures associated with significant fault zones characterized by fluid mixing and wall rock reactions. The relationship between first influences the deposition of gold in these systems and lower-order structures (Groves et al. 2003; Sillitoe and Thompson 1998).

In RIRGS, the halo is characterized by a transition from proximal potassic alteration to phyllic and distal propylitic

alteration (Sillitoe and Thompson 1998). The alteration assemblages, commonly including K-feldspar, albite, and sericite alteration, are often accompanied by carbonate (Thompson et al. 1999). Characteristic alteration halos in orogenic gold systems typically involve sericite, carbonate, and sulfide minerals. These characteristics indicate that these deposits originate from low-salinity, CO<sub>2</sub>-rich fluids, which are attributed to the involvement of metamorphic fluids (Groves 2019; Hart 2007; Thompson et al. 1999). Pathfinder elements such as As, Sb, and Au often accompany these fluids. The Salgueiro and Serrita areas are situated near plutons. In Serrita, a polymetallic association similar to distal, such as Ag-Pb, is present with gold mineralizations entering the granodiorite to trondjemitic bodies of the Serrita suite. In Salgueiro, gold occurrences are hosted within the Salgueiro pluton, which also has a granodioritic to trondjemitic composition. The metallic association is similar to the more proximal one, mainly when mineralizations occur in the enclosing schist, with As, Au, and Ag as metals.

In both areas, granites display coexisting sericitic and potassic alteration. Distal margins contain fine-grained white mica with rare fluorite. Toward quartz veins, feldspar is locally replaced by K-feldspar with perthitic textures and coarse muscovite at vein contacts; plagioclase shows sericitization. Adjacent to schists, carbonate, chlorite, sericite, and cordierite are present. The presence of paragonite in mineralized quartz veins near Salgueiro was interpreted as a product of magmatic-hydrothermal fluids (Noronha et al. 2024).

Gamma-ray spectrometric data indicate that potassium hydrothermalism has significantly altered the host rocks near mineralized areas (Oliveira et al. 2024). The 3D inversion of the magnetization vector reveals large magmatic bodies from the Serrita Suite, extending over 5 km in depth, with no induced or remanent magnetization (Oliveira et al. 2024). This assumption implies a low magnetic susceptibility, suggesting a magmatic influence with a low oxidation state, a key feature favorable in forming reduced intrusion-related gold systems (Hart 2007).

Although most mineralizations occur east of the Parnamirim Shear Zone, the study's advances present new occurrences to the west close to other shear systems, providing a fresh perspective on the area's geological dynamics.

Electrum, an Au-Ag alloy, is significant in hydrothermal systems as it is a petrogenetic indicator of ore-forming processes. It can provide valuable information about the conditions and mechanisms of ore deposition (Gammons and Williams-Jones 1995). Orogenic gold systems may exhibit preconcentration of Au relative to Ag, leading to fluids that form deposits with higher Au/Ag ratios (Gammons and Williams-Jones 1995).

In the vein deposits of the Salgueiro and Serrita areas, Ag-Au alloys with silver content reached up to 51wt.% may indicate variations in fluid compositions. This suggests that more than one fluid type is involved beyond the metamorphic fluid commonly inferred from the aqueous and aqueous-carbonic fluid types. These additional fluids could include magmatic or non-magmatic sources, possibly derived from wall rocks or circulating meteoric or connate fluids.

Pb-Pb isotopic values obtained from the whole rock of granites, schists, and mineral galena of the Serrita district (Barra Verde Mine) (Marinho 2012) show homogeneous values from granites compared to those found in the galena hosted in the veins cutting through them. In contrast, the same does

not occur in the Pb–Pb isotopic compositions for the galena and host schists, suggesting in part that metals such as lead could come from/carried out by the magmatic-hydrothermal source. Similar lead behavior between veins, batholiths, and wall rocks occurs in Au–As–Pb–Zn–Cu Parcoy–Pataz district, Peru, and Au–Te–Pb–Zn–Cu Dongping, Hebei province, China (Sillitoe and Thompson 1998).

In summary, hydrothermal halos such as potassic, phyllic, and sericitic surrounding mineralizations enclosed in granites; Ag–Au alloys; anomalous potassic with low magnetic susceptibility features suggesting reduced granites; Ag–Pb sheeted veins (distal?); and Pb–Pb isotopic data favors the contribution of magmatic-hydrothermal fluids; the aqueous-carbonic fluid inclusions with low salinity, high content of mercury, major shear zones close to some deposits, chlorite-carbonate halos in metasediments favor orogenic gold deposits at shallower emplacement at all.

We consider the scenario for the coexistence of free gold (in quartz veins) and inclusion-hosted gold (in pyrite, arsenopyrite, chalcopyrite) within contrasting alteration assemblages (proximal potassic-like K-feldspar-quartz-muscovite in granite vs. chlorite-carbonate in metasediments) to a contemporaneous interaction between a magmatic-hydrothermal fluid exsolved from reduced intrusions and a metamorphic-orogenic fluid contributed by the surrounding supracrustal pile, promoting gold precipitation at the vein scale. The spatial juxtaposition of free and inclusion-hosted gold within the same vein sets, together with K-rich halos and Hg-bearing electrum, favors a syn-mineral, mixing-dominated model at epizonal depth. We frame this as a working hypothesis pending targeted fluid-inclusion and isotope studies to resolve timing and sources (cf. Groves et al. 2003; Lang and Baker 2001; Goldfarb and Pitcairn 2023).

## 7. Conclusions

Field, petrographic, and microchemical data indicate two recurring vein architectures hosted by granites and metasediments, respectively, with vertical to subvertical quartz lodes arranged as sheets and local breccias. Alteration halos are systematically contrasted: K-feldspar-quartz-muscovite  $\pm$  rare fluorite potassic to phyllic-like assemblages in granites versus chlorite-carbonate  $\pm$  sericite  $\pm$  cordierite in metasediments. These patterns point to distinct thermal and fluid regimes linked to intrusive bodies and major shear zones.

Gold occurs as free particles in quartz and as inclusions in pyrite, chalcopyrite, arsenopyrite, hematite, and martite, with systematic domain-scale differences in fineness and Ag contents. Hg-bearing electrum and local Ag–Pb associations near granites are consistent with reduced, F-bearing magmatic-hydrothermal inputs, whereas chlorite-carbonate halos in metasediments align with shallow orogenic conditions. The spatial juxtaposition of free and inclusion-hosted gold within the same vein sets records for fluid evolution at the vein scale.

The integrated evidence suggests a hybrid, mixing-dominated model in which magmatic-hydrothermal fluids exsolved from reduced intrusions interacted with metamorphic-orogenic fluids in epizonal conditions, triggering gold precipitation

## Acknowledgments

The authors thank the companies Promining, Coogascen (Cooperativa dos Garimpeiros do Sertão Central), and Brandão & Simas Mineração for allowing access to the areas and exploration points; and the Geological Survey of Brazil for supporting and financing the research. We are immensely grateful for the enriching work of the anonymous reviewers.

## Authorship credits

Author	A	B	C	D	E	F
SBG						
GAL						
ALCC						
DAS						
FJCL						

A - Study design/ Conceptualization B - Investigation/ Data acquisition  
C - Data Interpretation/ Validation D - Writing  
E - Review/Editing F - Supervision/Project administration

## References

- Almeida F.F.M., Hasui Y., Brito Neves B.B., Fuck R.A. 1981. Brazilian structural provinces: an introduction. *Earth Science Reviews*, 17(1-2), 1-29. [https://doi.org/10.1016/0012-8252\(81\)90003-9](https://doi.org/10.1016/0012-8252(81)90003-9)
- Almeida H.L., Misas C.M.E., Teles G.S. 2024. Microfabric, 3D-strain geometry and kinematic vorticity analysis of Au-bearing shear zone, Central Domain of the Borborema Province, NE Brazil. *Journal of South American Earth Sciences*, 133, 104720. <https://doi.org/10.1016/j.jsames.2023.104720>
- Araújo M.N.C., Silva F.C.A., Jardim de Sá E.F., Holcombe R.J. 2002. Geometry and structural control of gold vein mineralizations in Seridó Belt, northeast Brazil. *Journal of South American Earth Science*, 15(3), 337-348. [https://doi.org/10.1016/S0895-9811\(02\)00040-8](https://doi.org/10.1016/S0895-9811(02)00040-8)
- Archânjo C.J., Fetter A.H. 2004. Emplacement setting of the granite sheeted pluton of Esperança (Brasiliano orogen, Northeastern Brazil). *Precambrian Research*, 135(3), 193-215. <https://doi.org/10.1016/j.precamres.2004.08.008>
- Archânjo C.J., Hollanda M.H. B., M., Rodrigues S.W., Brito Neves B.B., Armstrong R. 2008. Fabrics of pre- and syntectonic granite plutons and chronology of shear zones in the Eastern Borborema Province, NE Brazil. *Journal of Structural Geology*, 30(3), 310-326. <https://doi.org/10.1016/j.jsg.2007.11.011>
- Ateh K.I., Suh C.E., Shuster J., Shemang E.M., Vishiti A., Reith F., Southam G. 2021. Alluvial gold in the Bératé Oya drainage system, east Cameroon. *Journal of Sedimentary Environments*, 6, 201-212. <https://doi.org/10.1007/s43217-021-00051-w>
- Beurlen H., Silva M.R.R., Santos R.B. 1997. Auriferous quartz veins from Northeastern Brazil: a fluid-inclusion study. *International Geology Review*, 39(7), 578-588. <https://doi.org/10.1080/00206819709465289>
- Beurlen H. 1995. The mineral resources of the Borborema Province in Northeastern Brazil and its sedimentary cover: a review. *Journal of South American Earth Sciences*, 8(3-4), 365-376. [https://doi.org/10.1016/0895-9811\(95\)00020-G](https://doi.org/10.1016/0895-9811(95)00020-G)
- Black R., Latouche L., Liégeois J.P., Caby R., Bertrand J.M. 1994. Pan-African displaced terranes in the Tuareg shield (central Sahara). *Geology*, 22(7), 641-644. [https://doi.org/10.1130/0091-7613\(1994\)022%3C0641:PADTIT%3E2.3.CO;2](https://doi.org/10.1130/0091-7613(1994)022%3C0641:PADTIT%3E2.3.CO;2)
- Brito Neves B.B., Fuck R.A., Campanha G.A.C. 2021. Basement inliers of the Brasiliano structural provinces of South America. *Journal of South American Earth Sciences*, 110, 103392. <https://doi.org/10.1016/j.jsames.2021.103392>
- Brito Neves B.B., Van Schmus W.R., Campos Neto M.C. 2018. Sistema de dobramentos Piancó-Alto Brígida (PE-PB-CE), regionalização geotectônica e geocronologia. *Geologia USP, Série Científica*, 18(4), 149-171. <https://doi.org/10.11606/issn.2316-9095.v18-142182>
- Brito Neves B.B., Santos E.J., Fuck R.A., Santos L.C.M.L. 2016. A preserved early Ediacaran magmatic arc at the northernmost portion of

- the Transversal Zone central subprovince of the Borborema Province, Northeastern South America. *Brazilian Journal of Geology*, 46(4), 491-508. <https://doi.org/10.1590/2317-4889201620160004>
- Brito Neves B.B., Fuck R.A., Pimentel M.M. 2014. The Brasiliano collage in South America: a review. *Brazilian Journal of Geology*, 44(3), 493-518. <https://doi.org/10.5327/Z2317-4889201400030010>
- Brito Neves B.B., Van Schmus W.R., Kozuch M., Santos E.J., Petronilho L.A. 2005. Zona Tectônica Teixeira Terra Nova – ZTTTN: fundamentos da geologia regional e isotópica. *Geologia USP, Série Científica*, 5(1), 57-80. <https://doi.org/10.5327/S1519-874X2005000100005>
- Brito Neves B.B., Santos E.J., Van Schmus W.R. 2000. Tectonic history of the Borborema province. In: Cordani U.G., Milani E.J., Thomaz Filho A., Campos D.A. (eds.). *Tectonic evolution of South America*. Rio de Janeiro, 31st International Geological Congress, p. 151-182. Available online at: <https://rigeo.sgb.gov.br/handle/doc/19419> / (accessed on 29 October 2025).
- Brito Neves B.B., Van Schmus W.R., Santos E.J., Campos Neto M.C., Kozuch M. 1995. O evento Cariris Velhos na Província Borborena: integração de dados, implicações e perspectivas. *Revista Brasileira de Geociências*, 25(4), 279-296. <https://doi.org/10.25249/0375-7536.1995279296>
- Brito M.F.L., Marinho M.S. 2017. Geologia e recursos minerais da folha Salgueiro SC.24-V-B-III, estado de Pernambuco. Recife, CPRM, 207 p. Available online at: <https://rigeo.sgb.gov.br/handle/doc/17660> / (accessed on 29 October 2025).
- Caby R., Sial A.N., Ferreira V.P. 2009. High-pressure thermal aureoles around two Neoproterozoic synorogenic magmatic epidote-bearing granitoids, northeastern Brazil. *Journal of South American Earth Sciences*, 27(2-3), 184-195. <https://doi.org/10.1016/j.jsames.2008.09.005>
- Canedo G.F. 2016. Os depósitos Serrote da Laje e Caboclo (Cu-Au), nordeste do Brasil: sulfetos magmáticos hospedados em rochas ricas em magnetita e ilmenita associadas a intrusões máficas-ultramáficas. MSc Dissertation, Universidade de Brasília, Brasília, p. 57. <http://dx.doi.org/10.26512/2016.09.D.22354>
- Caxito F.A., Uhlein A., Dantas E.L. 2014b. The Afeição augen-gneiss Suite and the record of the Cariris Velhos Orogeny (1000–960 Ma) within the Riacho do Pontal fold belt, NE Brazil. *Journal of South America. Earth Sciences*, 51, 12–27. <https://doi.org/10.1016/j.jsames.2013.12.012>
- Caxito F.A., Uhlein A., Dantas E.L., Stevenson R., Salgado S.S., Dussan I.A., Sial A.N. 2016. A complete Wilson Cycle recorded within the Riacho do Pontal Orogen, NE Brazil: Implications for the Neoproterozoic evolution of the Borborema Province at the heart of West Gondwana. *Precambrian Research*, 282, 97–120. <https://doi.org/10.1016/j.precamres.2016.07.001>
- Caxito F.A., Uhlein A., Stevenson R., Uhlein G.J. 2014a. Neoproterozoic oceanic crust remnants in northeast Brazil. *Geology*, 42(5), 387-390. <https://doi.org/10.1130/G35479.1>
- Chapman J.B., Shields J.E., Ducea M.N., Paterson, S.R., Attia S., Ardill K.E. 2021. The causes of continental arc flare ups and drivers of episodic magmatic activity in Cordilleran orogenic systems. *Lithos*, 398-399, 106307. <https://doi.org/10.1016/j.lithos.2021.106307>
- Costa F.G. 2018. Geologia e metalogênese do ouro do greenstone belt da Serra das Pipocas, maciço de Troia, Província Borborema, NE-Brasil. PhD Thesis, Universidade Federal do Pará, Belém, 226 p. Available online at: <https://rigeo.sgb.gov.br/handle/doc/21218> / (accessed on 29 October 2025).
- Costa A.P., Dantas A.R. 2018. Geologia e recursos minerais da folha Lajes SB.24-X-D-VI, estado do Rio Grande do Norte: texto explicativo. Recife, CPRM, 163 p. Available online at: <http://rigeo.cprm.gov.br/jspui/handle/doc/20238> / (accessed on 29 October 2025).
- Costa F.G., Klein E.L., Galarza M.A., Pineo T.R.G. 2019. Structural features and age of gold mineralization in the Troia Massif, Borborema Province, NE Brazil: A Paleoproterozoic (~2029 Ma) hypozonal orogenic gold deposit overprinted by the late Neoproterozoic Brasiliano/Pan-African orogeny. *Journal of South American Earth Sciences*, 93, 119-139. <https://doi.org/10.1016/j.jsames.2019.05.003>
- Coutinho M.G.N. 1994. The Geology of the shear zone hosted gold deposits in Northeast Brazil. PhD Thesis, University of London, London, 391 p. Available online at: <https://rigeo.sgb.gov.br/handle/doc/111> / (accessed on 29 October 2025).
- Coutinho M.G.N., Alderton D.H.M. 1998. Proterozoic lode gold deposits in the Borborema Province NE Brazil and their exploration significance. *Anais Academia Brasileira de Ciências*, 70(3), 429-439. Available online at: <https://rigeo.sgb.gov.br/handle/doc/17069> / (accessed on 29 October 2025).
- Cruz R.F. 2015. Geologia e recursos minerais da folha Parnamirim: estado de Pernambuco. Recife, CPRM, 145 p. Available online at: <https://rigeo.sgb.gov.br/handle/doc/15951> / (accessed on 29 October 2025).
- Deng C., Sun G., Rong Y., Sun R., Sun D., Lehmann B., Yin R. 2021. Recycling of mercury from the atmosphere-ocean system into volcanic-arc-associated epithermal gold systems. *Geology*, 49 (3), 309–313. <https://doi.org/10.1130/G48132.1>
- Ferreira V.P., Sial A.N., Pimentel M.M., Moura C.A.V. 2004. Intermediate to acidic magmatism and crustal evolution in the Transversal Zone, Northeastern Brazil. In: Mantesso Neto V., Bartorelli A., Carneiro C.D.R., Brito Neves B.B. (eds.). *Geologia do continente sul-americano: a evolução da obra de Fernando Flávio de Almeida*. São Paulo, Editora Beca, p. 189-201. Available online at: <http://sbg.sitepessoal.com/livrosadobados/geologiaSul.pdf> / (accessed on 29 October 2025).
- Figueiredo B.R. 1995. Contrastes mineralógicos e químicos entre os complexos máfico-ultramáficos mineralizados a cobre do R/22 Caraíba (BA) e do Serrote da Lage (AL). In: Congresso Brasileiro de Geoquímica, 3, 621-623. Available online at: <https://www.sbgq.org.br/anais-dos-congressos/> / (accessed on 29 October 2025).
- Gammons C.H., Williams-Jones A.E. 1995. Hydrothermal geochemistry of electrum; thermodynamic constraints. *Economic Geology*, 90(2), 420-432. <https://doi.org/10.2113/gsecongeo.90.2.420>
- Ganade C.E., Weinberg R.F., Caxito F.A., Lopes L.B.L., Tesser R., Costa I.S. 2021. Decratonization by rifting enables orogenic reworking and transcurent dispersal of old terranes in NE Brazil. *Nature Scientific Reports*, 11, 5719. <https://doi.org/10.1038/s41598-021-84703-x>
- Ganade C.E., Weinberg R.F., Cordani U.G. 2014. Extruding the Borborema Province (NE-Brazil): a two-stage Neoproterozoic collision process. *Terra Nova*, 26(2), 157-168. <https://doi.org/10.1111/ter.12084>
- Ganade C.E., Cordani U.G., Agbossoumounde Y., Caby R., Basei M.A.S., Weinberg R.F., Sato K. 2016. Tightening-up NE Brazil and NW Africa connections: new U-Pb/Lu-Hf zircon data of a complete plate tectonic cycle in the Dahomey belt of the West Gondwana Orogen in Togo and Benin. *Precambrian Research*, 276, 24–42. <https://doi.org/10.1016/j.precamres.2016.01.032>
- Goldfarb R.J., Pitcairn I. 2023. Orogenic gold: is a genetic association with magmatism realistic? *Mineralium Deposita*, 58(1), 5-35. <https://doi.org/10.1007/s00126-022-01146-8>
- Goldfarb R.J., Groves D.I. 2015. Orogenic gold: Common or evolving fluid and metal sources through time. *Lithos*, 233, 2–26. <https://doi.org/10.1016/j.lithos.2015.07.011>
- Goldfarb R.J., Groves D.I., Gardol S. 2001. Orogenic gold and geologic time: a global synthesis. *Ore Geology Reviews*, 18(1-2), 1-75. [https://doi.org/10.1016/S0169-1368\(01\)00016-6](https://doi.org/10.1016/S0169-1368(01)00016-6)
- Groves D.I. 2019. Orogenic gold deposits: part of a global dynamic conjunction between subduction and gold. *Exploration Geophysics*, 2019(1), 1-3. <https://doi.org/10.1080/22020586.2019.12073249>
- Groves D.I., Goldfarb, R.J., Robert F., Hart C.J.R. 2003. Gold deposits in metamorphic belts: overview of current understanding, outstanding problems, future research, and exploration significance. *Economic Geology*, 98(1), 1–29. <https://doi.org/10.2113/gsecongeo.98.1.1>
- Groves D.I., Goldfarb R.J., Gebre-Mariam M., Hagemann S.G., Robert F. 1998. Orogenic gold deposits: a proposed classification in the context of their crustal distribution and relationship to other gold deposit types. *Ore Geology Reviews*, 13(1-5), 7-27. [https://doi.org/10.1016/S0169-1368\(97\)00012-7](https://doi.org/10.1016/S0169-1368(97)00012-7)
- Groves D.I., Santosh M., Goldfarb R.J., Zhang L. 2018. Structural geometry of orogenic gold deposits: implications for exploration of world-class and giant deposits. *Geoscience Frontiers*, 9(4), 1163-1177. <https://doi.org/10.1016/j.gsf.2018.01.006>
- Guimarães I.P., Silva Filho A.F., Almeida C.N., Van Schmus W.R., Araújo J.M.M., Melo S.C., Melo E.B. 2004. Brasiliano (Pan-African) granitic magmatism in the Pajeú-Paraíba belt, Northeast Brazil: an isotopic and geochronological approach. *Precambrian Research*, 135(1-2), 23-53. <https://doi.org/10.1016/j.precamres.2004.07.004>
- Hart C.J.R. 2007. Reduced Intrusion -Related Gold Systems. In: Goodfellow W.D. (ed.). *Mineral deposits of Canada: a synthesis of major deposit types, District Metallogeny, the evolution of geological provinces, and exploration methods*. Special Publication, 5, Geological Association of Canada, p. 95–112. <https://doi.org/10.2113/gsecongeo.102.7.1355>
- Hollanda M.H.B.M., Archanjo C.J., Souza L.C., Armstrong R., Vasconcelos P.M. 2010. Cambrian mafic to felsic magmatism and its connections with transcurent shear zones of the Borborema Province (NE Brazil): implications for the late assembly of the West Gondwana. *Precambrian Research*, 178(1-4), 1-14. <https://doi.org/10.1016/j.precamres.2009.12.004>



- Hollanda M.H.B.M., Souza Neto J.A.S., Archanjo J.C., Stein H., Maia A.C. 2017. Age of the granitic magmatism and the W-Mo mineralization in skarns of the Seridó belt (NE Brazil) based on zircon U-Pb (SHRIMP) and molybdenite Re-Os dating. *Journal of South American Earth Sciences*, 79, 1–11. <https://doi.org/10.1016/j.jsames.2017.07.011>
- Horbach R., Marimon M.P.C. 1988. O depósito de cobre do Serrote da Laje, em Arapiraca, Alagoas. In: Congresso Brasileiro de Geologia, 35, 1, 1–15. Available online at: <http://www.sbgeo.org.br/home/pages/44> / (accessed on 29 October 2025).
- Hough R.M., Butt C.R.M., Fischer-Bühner J. 2009. The crystallography, metallography and composition of gold. *Elements*, 5(5), 297–302. <https://doi.org/10.2113/gselements.5.5.297>
- Jardim de Sá E.F., Macedo M.H.F., Fuck R.A., Kawashita K. 1992. Terrenos proterozóicos na Província Borborema e a margem norte do Cráton São Francisco. *Revista Brasileira de Geociências*, 22(4), 472–480. <https://doi.org/10.25249/0375-7536.1991472480>
- Ketchaya Y.B., Dong G., Santosh M., Lemdjou Y.B. 2022. Microchemical signatures of placer gold grains from the Gamba district, northern Cameroon: implications for possible bedrock sources. *Ore Geology Reviews*, 141, 104640. <https://doi.org/10.1016/j.oregeorev.2021.104640>
- Klein E., Queiroz L.C., Silva A.R.C., Oliveira A.C., Basto C.F., Oliveira C.E., Chaves C.L., Silva C.M.G., Alves C.L., Miranda D., Palheta E., Costa F.G., Lima F.J.C., Rios F.S., Marques I.P., Laux J.H., Marinho M.S. 2024. A design of gold-bearing metallogenic provinces and districts in Brazil. *Journal of the Geological Survey of Brazil*, 7(2), 165–171. <https://doi.org/10.29396/jgsb.2024.v7.n2.5>
- Kosin M.D., Angelim L.A.A., Souza J.D., Guimarães J.T., Teixeira L.R., Martins A.A.M., Bento R.V., Santos R.A., Vasconcelos A.M., Neves J.P., Wanderley A.A., Carvalho L.M., Pereira L.H.M., Gomes I.P. 2004. Carta geológica do Brasil ao milionésimo: Aracaju: folha SC.24, Escala 1:1.000.000. Programa Geologia do Brasil, Brasília, CPRM. Available online at: <https://rigeo.sgb.gov.br/handle/doc/4985> / (accessed on 29 October 2025).
- Lages G.A., Marinho M.S., Nascimento M.A.L., Medeiros V.C., Dantas E.L. 2016. Geocronologia e aspectos estruturais e petrológicos do Pluton Bravo, Domínio Central da Província Borborema, Nordeste do Brasil: um granito transalcalino precoce no estágio pós-colisional da Orogênese Brasileira. *Brazilian Journal of Geology*, 46(1), 41–61. <https://doi.org/10.1590/2317-4889201620150033>
- Lang J., Baker T. 2001. Intrusion-related gold systems: the present level of understanding. *Mineralium Deposita*, 36(6), 477–489. <https://doi.org/10.1007/s001260100184>
- Liégeois J.P., Black R., Navez J., Latouche L. 1994. Early and late Pan-African orogenies in the Aïr assembly of terranes (Tuareg shield, Niger). *Precambrian Research*, 67(1–2), 59–88. 1994. [https://doi.org/10.1016/0301-9268\(94\)90005-1](https://doi.org/10.1016/0301-9268(94)90005-1)
- Liégeois J.P., Latouche L., Boughrara M., Navez J., Guiraud M. 2003. The Latea metacraton (Central Hoggar, Tuareg shield, Algeria): behavior of an old passive margin during the Pan-African orogeny. *Journal of African Earth Science*, 37(3–4), 161–190. <https://doi.org/10.1016/j.jafrearsci.2003.05.004>
- Liu H., Beaudoin G. 2021. Geochemical signatures in native gold derived from Au-bearing ore deposits. *Ore Geology Reviews*, 132, 104066. <https://doi.org/10.1016/j.oregeorev.2021.104066>
- Lopez J.M. 2012. Programa de exploração mineral do grupo Jaguar Mining Inc. In: Simpósio de Exploração Mineral, SIMEXMIN. Available online at: <https://pt.scribd.com/document/502189763/Jaguarisgold-Simexmin-Programa-de-Exploracao-Mineral-Do-Grupo-Jaguar-Mining-Inc-Jean-marc-Lopez-Maio-2012> / (accessed on 31 October 2025).
- Marinho M.S. 2012. Evolução estrutural e aspectos petrológicos das ocorrências auríferas de Serrita e Parnamirim, Pernambuco. MSc Dissertation, Universidade Federal de Ouro Preto, Ouro Preto, 143 p. Available online at: <http://www.repositorio.ufop.br/handle/123456789/2972> / (accessed on 29 October 2025).
- Marinho M.S., Gomes C.J.S. 2013. Structural evolution of Au, Ag, and Pb lode occurrences of Serrita and Parnamirim, Pernambuco, Brazil. *Brazilian Journal of Geology*, 43(2), 211–222. <https://doi.org/10.5327/Z2317-48892013000200002>
- Medeiros V.C. 2004. Evolução geodinâmica e condicionamento estrutural dos terrenos Piauçu - Alto Brígida e Alto Pajeú, domínio da zona transversal, NE do Brasil. PhD Thesis, Universidade Federal do Rio Grande do Norte, Natal, 199 p. Available online at: <https://rigeo.sgb.gov.br/handle/doc/105> / (accessed on 29 October 2025).
- Mont'Alverne A.A.F., Anjos F.T., Cintra J.R.F., Dantas J.R.A., Santos R.B., Souza V.C. 1995. Projeto Serrita-Cedro, Fase I. Recife, DNPM, 29 p. Available online at: <https://rigeo.sgb.gov.br/handle/doc/24999> / (accessed on 29 October 2025).
- Morrison G.W., Rose W.J., Jaireth S. 1991. Geological and geochemical controls on the silver content (fineness) of gold in gold–silver deposits. *Ore Geology Reviews*, 6(4), 333–364. [https://doi.org/10.1016/0169-1368\(91\)90009-V](https://doi.org/10.1016/0169-1368(91)90009-V)
- Naumov V.B., Dorofeeva V.A., Mironova O.F. 2018. Physicochemical parameters of the origin of hydrothermal mineral deposits: evidence from fluid inclusions. V. Antimony, Arsenic, and Mercury deposits. *Geochemistry International*, 56(9), 901–914. <https://doi.org/10.1134/S0016702918090082>
- Neves S.P. 1986. Petrologia e geoquímica dos stocks graníticos de Serrita, Pernambuco. *Revista Brasileira de Geociências*, 16(1), 86–94. Available online at: <https://papegeo.igc.usp.br/portal/index.php/rbg/petrologia-e-geoquimica-dos-stocks-graniticos-de-serrita-pernambuco/> / (accessed on 29 October 2025).
- Neves S.P. 1988. Intrusão diápirica, cristalização e deformação: stocks graníticos de Serrita, Pernambuco. In: Congresso Brasileiro de Geologia, 35, 3, 988–1003. Available online at: <http://www.sbgeo.org.br/home/pages/44> / (accessed on 31 October 2025).
- Neves S.P. 2003. Proterozoic history of the Borborema province (NE Brazil): Correlations with neighboring cratons and Pan-African belts and implications for the evolution of western Gondwana. *Tectonics*, 22(4), 1031. <https://doi.org/10.1029/2001TC001352>
- Neves S.P. 2015. Constraints from zircon geochronology on the tectonic evolution of the Borborema Province (NE Brazil): a widespread intracontinental Neoproterozoic reworking of a Paleoproterozoic accretionary orogen. *Journal of South America Earth Sciences*, 58, 150–164. <https://doi.org/10.1016/j.jsames.2014.08.004>
- Neves S.P., Mariano G. 1999. Assessing the tectonic significance of a large-scale transcurrent shear zone system: the Pernambuco lineament, northeastern Brazil. *Journal of Structural Geology*, 21(10), 1369–1383. [https://doi.org/10.1016/S0191-8141\(99\)00097-8](https://doi.org/10.1016/S0191-8141(99)00097-8)
- Neves S.P., Mariano G., Correia P.B., Silva, J.M.R. 2006. 70 m.y. of synorogenic plutonism in eastern Borborema Province (NE Brazil): temporal and kinematic constraints on the Brasiliano Orogeny. *Geodinamica Acta*, 19(3–4), 213–236. <https://doi.org/10.3166/ga.19.213-236>
- Neves S.P., Teixeira C.M.L., Brughier O. 2021. 870–850 Ma-old magmatic event in eastern Borborema Province, NE Brazil: Another Tonian failed attempt to break up the São Francisco Paleoplate? *Journal of South America Earth Sciences*, 105, 102917. <https://doi.org/10.1016/j.jsames.2020.102917>
- Neves S.P., Vauchez A., Feraud G. 2000. Tectono-thermal evolution magma emplacement, and shear zone development in the Caruaru area (Borborema Province, NE Brazil). *Precambrian Research*, 99(1–2), 1–32. [https://doi.org/10.1016/S0301-9268\(99\)00026-1](https://doi.org/10.1016/S0301-9268(99)00026-1)
- Neves S.P., Vauchez A. 1995. Magma emplacement and shear zone nucleation and development in northeast Brazil (Fazenda Nova and Pernambuco shear zones, State of Pernambuco). *Journal of South American Earth Sciences*, 8(3–4), 289–298. [https://doi.org/10.1016/0895-9811\(95\)00014-7](https://doi.org/10.1016/0895-9811(95)00014-7)
- Noronha D.D., Souza S.R.C., Pitombeira J.P.A. 2024. Geologia e potencial metalogenético para ouro de uma área ao norte do município de Salgueiro (PE). *Estudos Geológicos*, 33(1), 46–69. <https://doi.org/10.51359/1980-8208.2023.259797>
- Oliveira R.G., Rodrigues M.A.C., Domingos N.R.R., Silva E.P. 2024. Interpretação e modelagem de dados geofísicos do projeto avaliação do potencial mineral do oeste de Pernambuco para ouro e metais base. Recife, CPRM, 56 p. Available online at: <https://rigeo.sgb.gov.br/handle/doc/24938> / (accessed on 30 October 2025).
- Omang B.O., Suh C.E., Lehmann B., Vishiti A., Chombong N.N., Fon A.N., Egbe J.A., Shemang E.M. 2015. Microchemical signature of alluvial gold from two contrasting terrains in Cameroon. *Journal of African. Earth Science*. 112(Part A), 1–14 <https://doi.org/10.1016/j.jafrearsci.2015.09.004>
- Palacios C., Herail G., Townley B., MaksaeV V., Sepulveda F., Parseval P., Rivas P., Lahsen A., Parada M.A. 2001. The composition of gold in the Cerro Casale gold-rich porphyry deposit, Maricunga belt, northern Chile. *Canadian Mineralogist*, 39(3), 907–915. <https://doi.org/10.2113/gscanmin.39.3.907>
- Ridley J.R., Diamond L.W. 2000. Fluid chemistry of orogenic lode gold deposits and implications for genetic models. In: Hagemann S.G.,

- Brown P.E. (eds.). Gold in 2000. Society of economic geologists, reviews in economic geology, 13, 141-162. <https://doi.org/10.5382/Rev.13.04>
- Santos C.A., Pereira C.S., Palmeira L.C.M., Lima F.J.C., Lages G.A., Cunha A.L.C., Brito M.F.L., Santos R.B. 2021. Avaliação do potencial mineral do Oeste de Pernambuco para ouro e metais base, estados de Pernambuco e Ceará, mapa geológico, Escala 1:250.000. Recife, Serviço Geológico do Brasil. Available online at: <https://rigeo.sgb.gov.br/handle/doc/20474> / (accessed on 30 October 2025).
- Santos E.J. 1996. Ensaio preliminar sobre terrenos e tectônica acrescionária na Província Borborema. In: Congresso Brasileiro de Geologia, 39, 6, 47-50. Available online at: <http://www.sbgeo.org.br/home/pages/44> / (accessed on 30 October 2025).
- Santos E.J. 1995. O complexo granítico Lagoa das Pedras: acreção e colisão na região de Floresta (Pernambuco), Província Borborema. PhD These, Instituto de Geociências, Universidade de São Paulo, São Paulo, 219 p. <https://doi.org/10.11606/T.44.1995.tde-28102015-094036>
- Santos E.J., Medeiros V.C., 1999. Constraints from granitic plutonism on Proterozoic crustal growth of the Transverse Zone, Borborema Province, Northeast Brazil. Revista Brasileira de Geociências, 29(1), 73-84. Available online at: <https://ppegeo.igc.usp.br/portal/wp-content/uploads/tainacan-items/15906/41962/11154-13549-1-SM.pdf> / (accessed on 30 October 2025).
- Santos E.J., Souza Neto A.J., Silva M.R.R., Beurlen H., Cavalcanti J.A.D., Silva M.G., Dias V.M., Costa A.F., Santos L.C.M.L., Santos R.B. 2014. Metalogênese das porções norte e central da Província Borborema. In: Silva M.G., Rocha Neto M.B., Jost H., Kuyumjian R. Metalogênese das províncias tectônicas brasileiras. Belo Horizonte, CPRM, p. 343-388. Available online at: <https://rigeo.sgb.gov.br/handle/doc/19389> / (accessed on 30 October 2025).
- Santos E.J., Van Schmus W.R., Kozuch M., Brito Neves B.B. 2010. The Cariris Velhos tectonic event in northeast Brazil. Journal of South American Earth Sciences, 29(1), 61-76. <https://doi.org/10.1016/j.jsames.2009.07.003>
- Santos L.C.M.L., Dantas E.L., Cawood P.A., Santos E.J., Fuck R.A. 2017. Neoarchean crustal growth and Paleoproterozoic reworking in the Borborema Province, NE Brazil: insights from geochemical and isotopic data of TTG and metagranitic rocks of the Alto Moxotó Terrane. Journal of South American Earth Sciences, 79, 342-363. <https://doi.org/10.1016/j.jsames.2017.08.013>
- Sial A.N. 1986. Granite types in northeast Brazil: current knowledge. Revista Brasileira de Geociências, 16(1), 54-72. Available online at: <https://ppegeo.igc.usp.br/portal/index.php/rbg/granitetypes-in-northeast-brazil-current-knowledge> / (accessed on 30 October 2025).
- Sial A.N., Ferreira V.P. 2016. Magma associations in Ediacaran granitoids of the Cachoeirinha – Salgueiro and Alto Pajeú terranes, northeastern Brazil: forty years of studies. Journal of South American Earth Sciences, 68, 113-133. <https://doi.org/10.1016/j.jsames.2015.10.005>
- Sillitoe R.H., Thompson F.H. 1998. Intrusion-related vein gold deposits types tectono-magmatic settings and difficulties of distinction from orogenic gold deposits. Resource Geology, 48(4), 237-250. <https://doi.org/10.1111/j.1751-3928.1998.tb00021.x>
- Silva A.I., Souza S.R.C., Souza Neto J.A., Noronha D.D. 2024. Mapeamento geológico na área da mineralização aurífera (veio da prata e veio da ilha), a leste de Salgueiro (Pernambuco), Província Borborema, nordeste do Brasil. Estudos Geológicos, 34(1), 43-67. <https://doi.org/10.51359/1980-8208.2024.264087>
- Silva A.I. 2023. Estudo petrográfico e de química mineral de rochas mineralizadas em ouro, a leste de Salgueiro (Pernambuco), Província Borborema, nordeste do Brasil. Graduation work, Universidade Federal de Pernambuco.
- Silva J.M.R., Mariano G. 2000. Geometry and kinematics of the Afogados da Ingazeira shear zone, Northeast Brazil. International Geology Review, 42(1), 86-95. <https://doi.org/10.1080/00206810009465071>
- Silva Filho M.A. 1984. A faixa de dobramento Piancó: síntese do conhecimento e novas considerações. In: Congresso Brasileiro de Geologia, 33, 3337-3347.
- Souza Neto J.A., Legrand J.M., Volfinger M., Pascal M.L., Sonnet P. 2008. W–Au skarns in the Neo-Proterozoic Seridó Mobile Belt, Borborema Province in northeastern Brazil: an overview with emphasis on the Bonfim deposit. Mineralium Deposita, 43(2), 185-205. <https://doi.org/10.1007/s00126-007-0155-1>
- Thompson J.F.H., Sillitoe R.H., Baker T.R., Lang J.R., Mortensen J.K. 1999. Intrusion-related gold deposits associated with tungsten-tin provinces. 34(4), 323-334. <https://doi.org/10.1007/S001260050207>
- Torres H.H.F., Barros F.A.R., Santos E.J., Farina M., Maranhão R.J.L. 1986. Projeto Serrita: relatório final de pesquisa, Alvarás 3176/85, 4193/85, 4910/85 e 27 50/86. Recife, CPRM, 1 v.
- Torres H.H.F., Santos E.J. 1983. Projeto Serrita: atividades desenvolvidas em 1982 e programação para 1983. Recife, CPRM. 30 p. Available online at: <https://rigeo.sgb.gov.br/handle/doc/2023> / (accessed on 31 October 2025).
- Townley B.K., Hérail G., Maksaev V., Palacios C., Parseval P., Sepúlveda F., Orellana R., Rivas P., Ulloa C. 2003. Gold grain morphology and composition as an exploration tool: application to gold exploration in covered areas. Geochemistry: Exploration, Environment, Analysis, 3, 29-38. <https://doi.org/10.1144/1467-787302-042>
- Van Schmus W.R., Oliveira E.P., Silva Filho A.F., Toteu F., Penaye J., Guimarães I.P. 2008. Proterozoic links between the Borborema Province, NE Brazil, and the Central African Fold Belt. Journal of the Geological Society, 294(1), 69-99. <https://doi.org/10.1144/SP294.5>
- Van Schmus W.R., Kozuch M., Brito Neves B.B. 2011. Precambrian history of the Zona Transversal of the Borborema Province, NE Brazil: Insights from Sm-Nd and U-Pb geochronology. Journal of Geotechnical Earthquake Engineering, 31(2-3), 227-252. <https://doi.org/10.1016/j.jsames.2011.02.010>
- Vauchez A., Egydio-Silva M. 1992. Termination of a continental-scale strike-slip fault in partially melted crust: the West-Pernambuco shear zone, northeast Brazil. Geology, 20(11), 1007-1010. [https://doi.org/10.1130/0091-7613\(1992\)020%3C1007:TOACSS%3E2.3.CO;2](https://doi.org/10.1130/0091-7613(1992)020%3C1007:TOACSS%3E2.3.CO;2)
- Vauchez A., Neves S.P., Caby R., Corsini M., Egydio-Silva M., Arthaud M., Amaro V. 1995. The Borborema shear zone system, NE Brazil. Journal of South American Earth Sciences, 8(3-4), 247-266. [https://doi.org/10.1016/0895-9811\(95\)00012-5](https://doi.org/10.1016/0895-9811(95)00012-5)
- Yin X., Zhao X., Yin R., Gao L., Deng C., Tian Z., Chang S., Lehmann B. 2023. Mercury isotopic compositions of iron oxide-copper-gold (IOCG) hydrothermal systems: Deep Hg cycling in intracontinental settings. Chemical Geology, 641, 121777. <https://doi.org/10.1016/j.chemgeo.2023.121777>